Run #6: 1200°F with 7.83 vol% H_2S

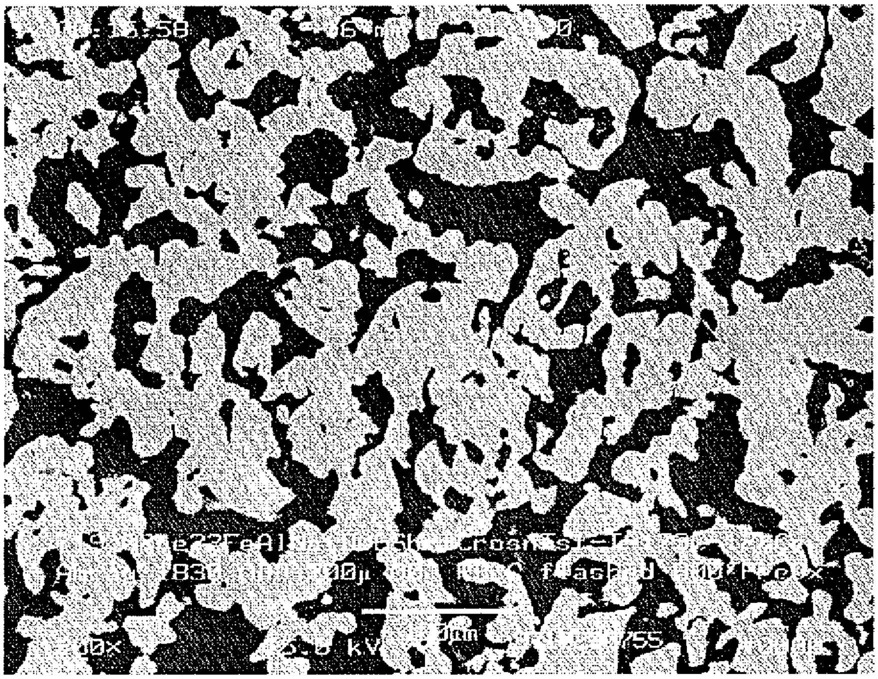

Figure 129: FAS, 800°C preoxidation, cross-section. 200X (T-173-C-1)

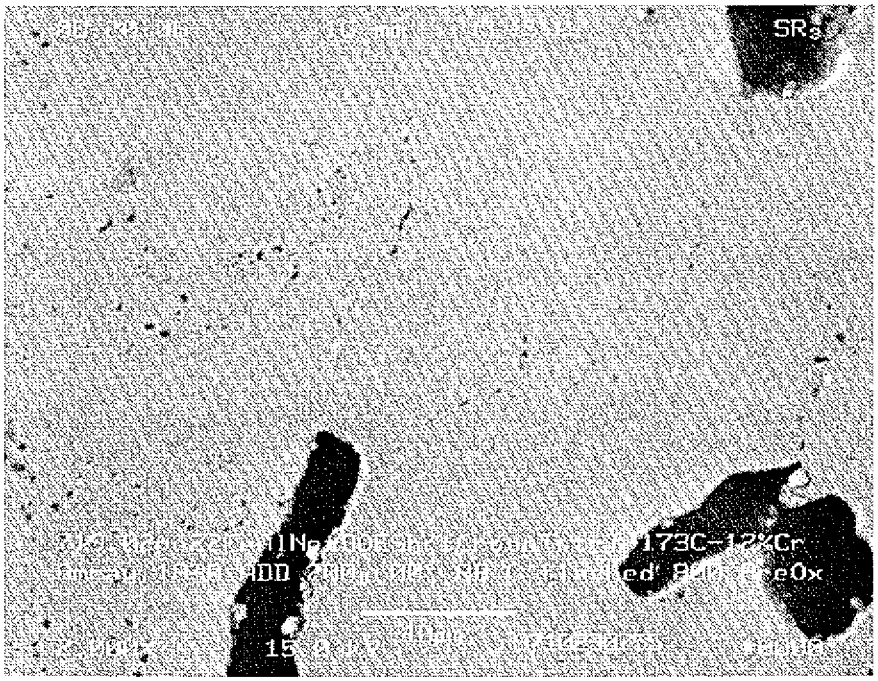

Figure 130: FAS, 800°C preoxidation, cross-section. 2000X (T-173-C-1)

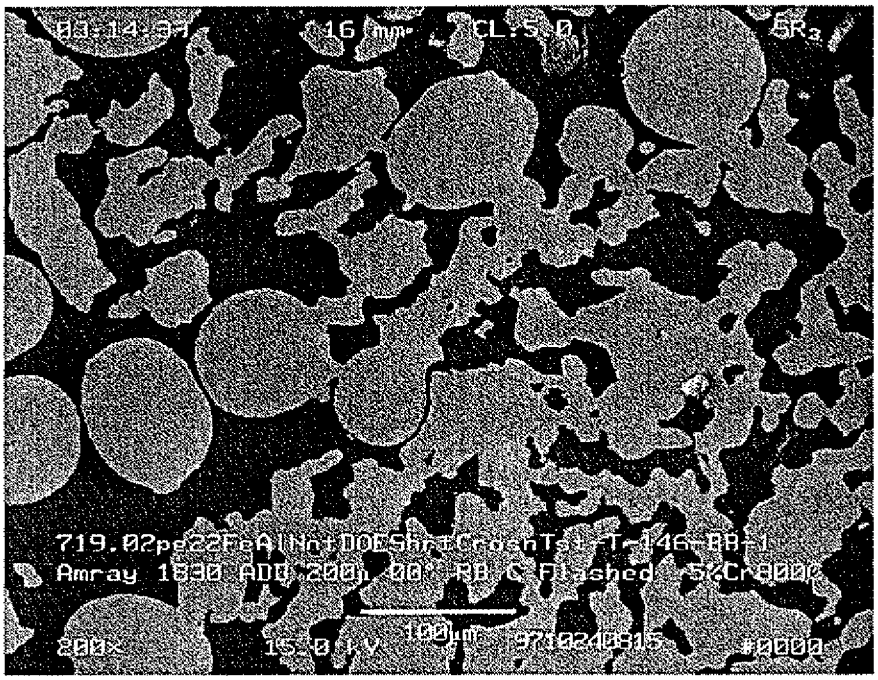

Figure 131: FAL, 800°C preoxidation, cross-section. 200X (T-146-BB-1)

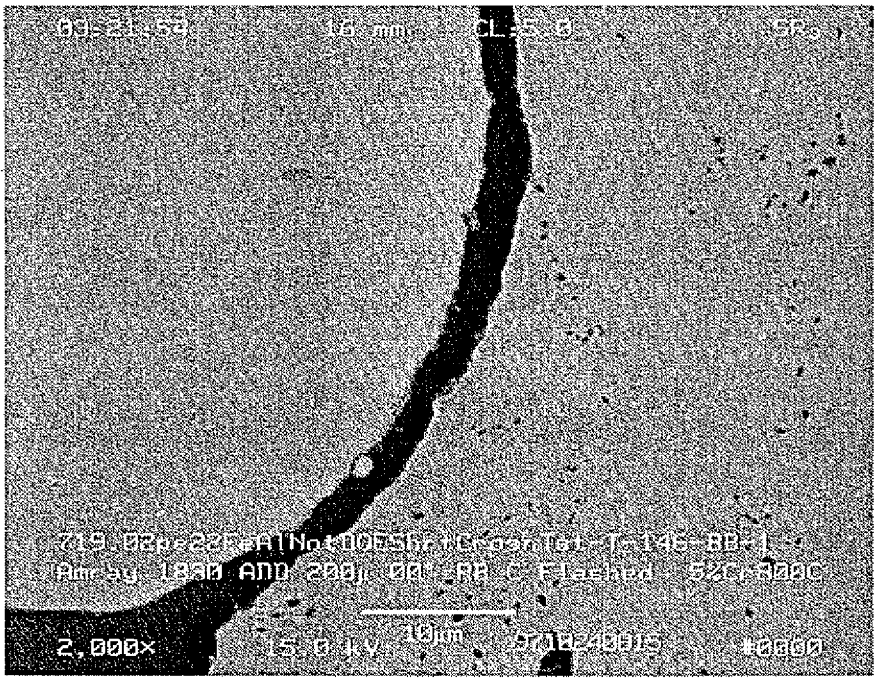

Figure 132: FAL, 800°C preoxidation, cross-section. 2000X (T-146-BB-1)

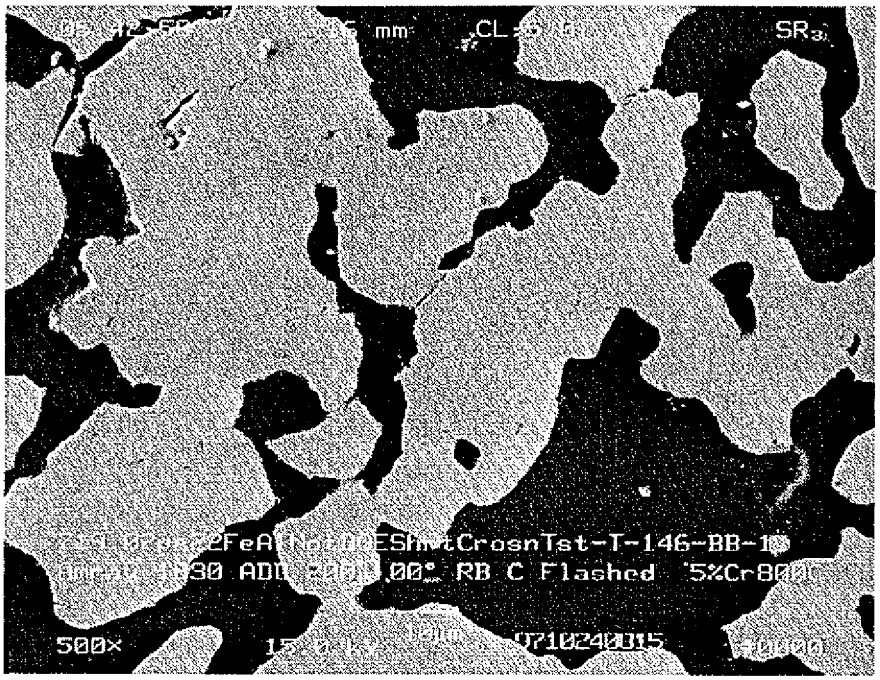

Figure 133: FAL, 800°C preoxidation, cross-section. Fractured sinter bonds, mechanical failure. 500X (T-146-BB-1)

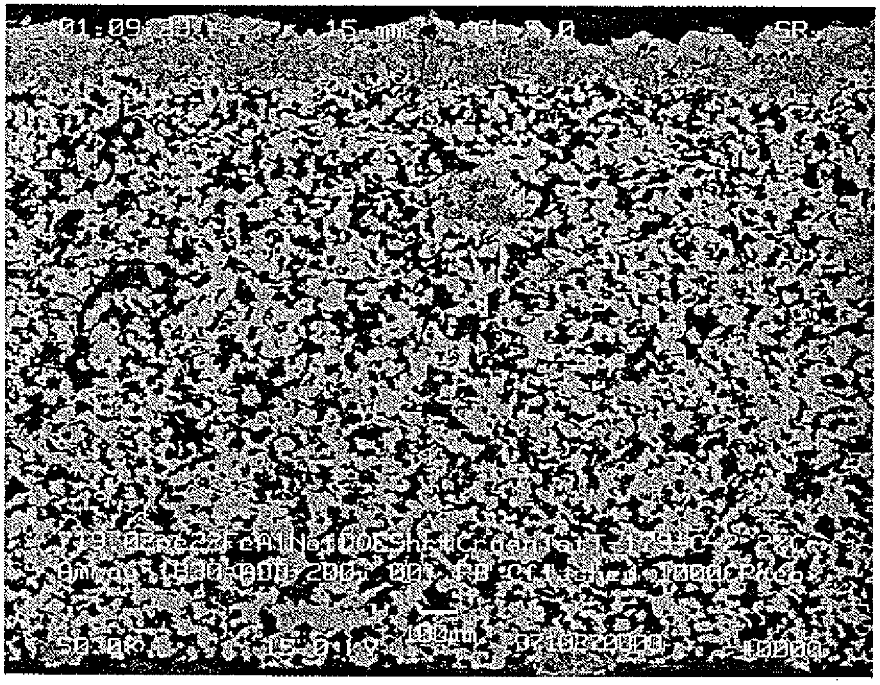

Figure 134: FAS, 1000°C preoxidation, cross-section. Corrosion product sealing pores. 50X (T-173-C-2)

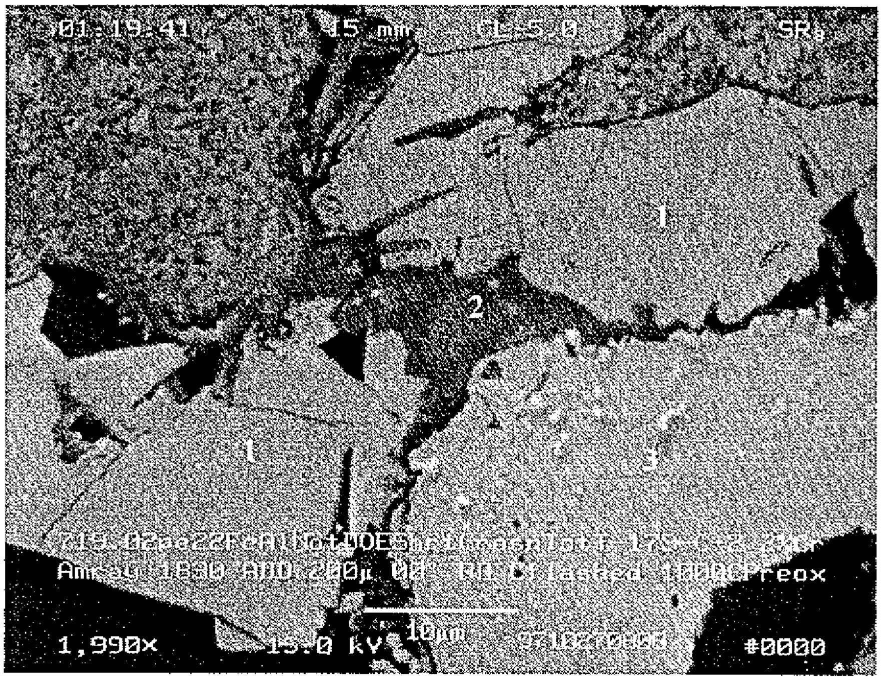

Figure 135: FAS, 1000°C preoxidation, cross-section. Sulfidation. Qualitative analysis on designated areas follow. 2000X (T-173-C-2)

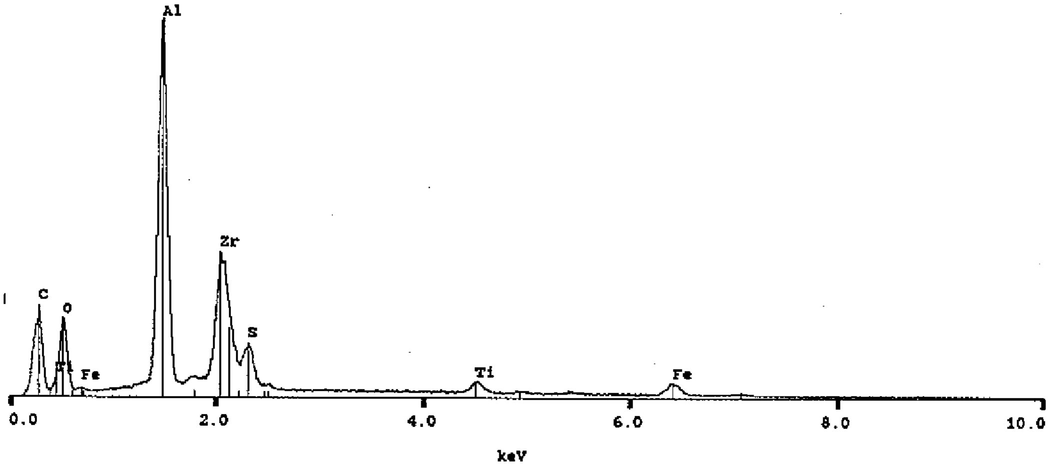

Figure 136: EDS spectrum of light contaminate (1) layer of Figure 135. Possibly Al_2O_3 - ZrO_2.

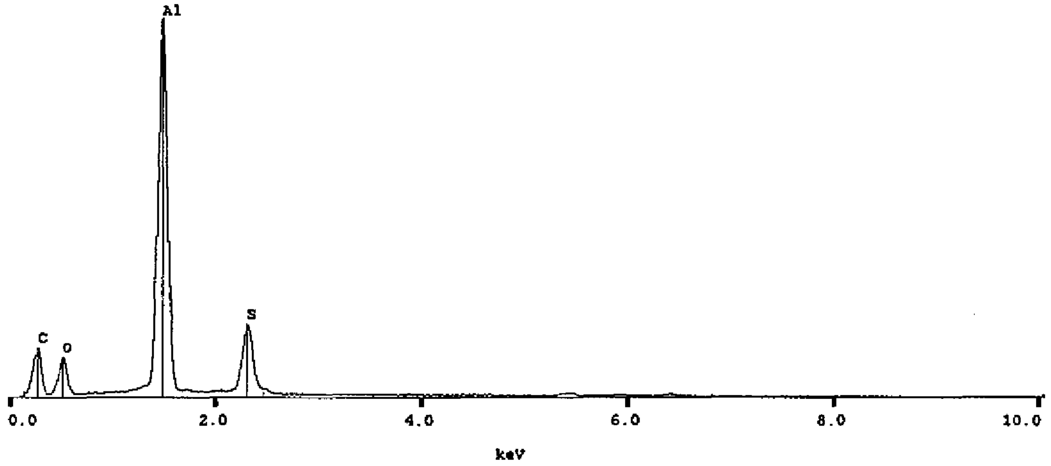

Figure 141: EDS spectrum of dark area of Figure 140. Alumina with sulfur.

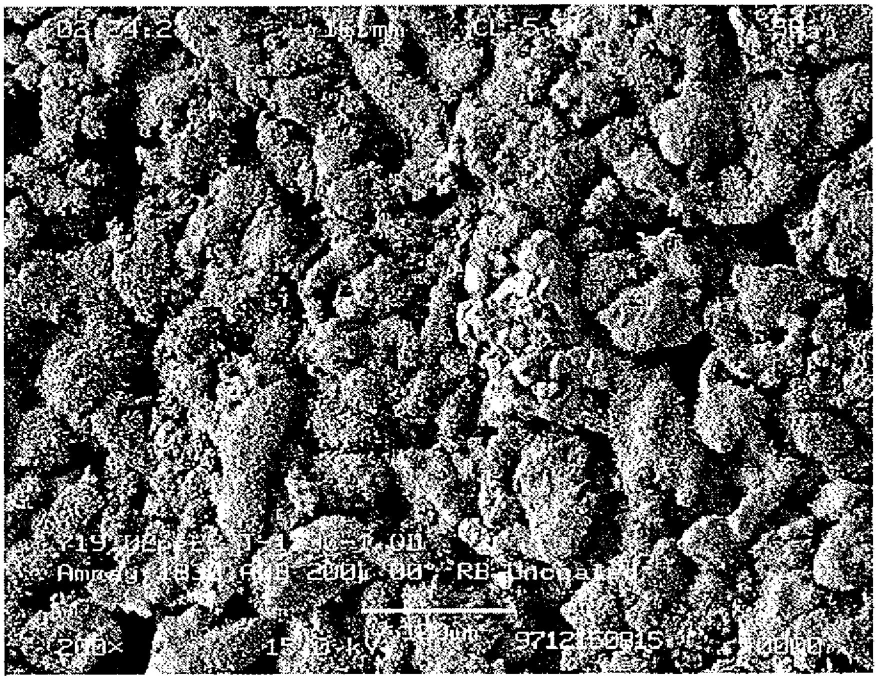

Figure 142: FAS, 800°C preoxidation, upstream surface of media. Crystal has high sulfur and iron (possible iron sulfide). 200X (T-173-C-1)

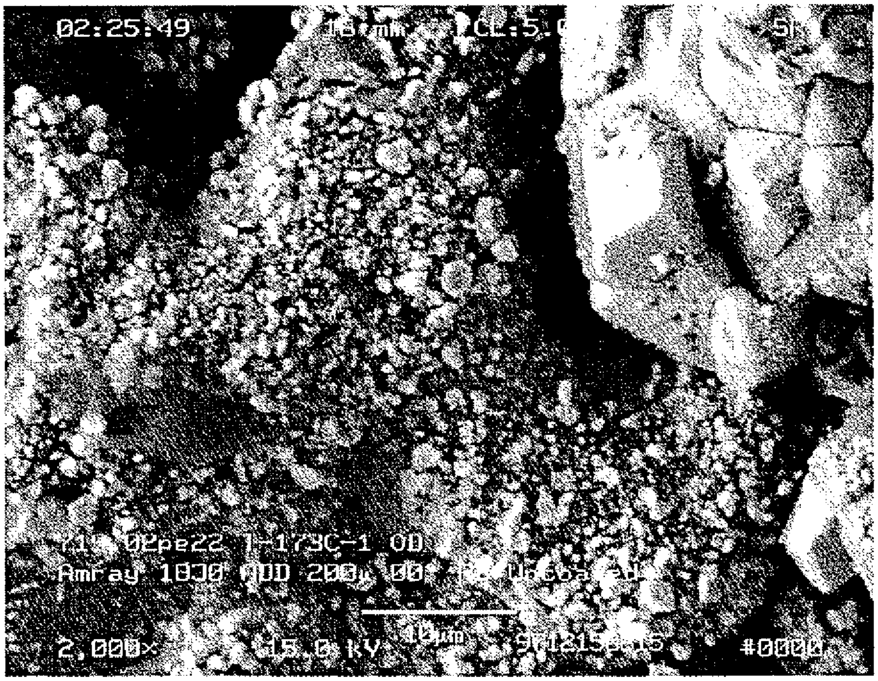

Figure 143: FAS, 800°C preoxidation, upstream surface of media. Sulfur detected with full screen spectrum. Covered with small crystals similar to the larger one. 2000X. (T-173-C-1)

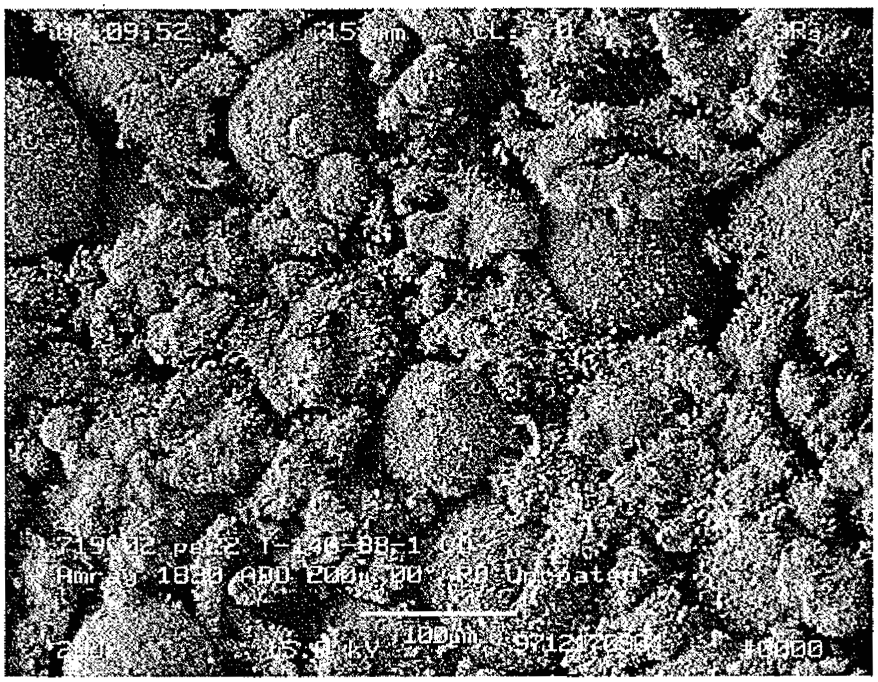

Figure 144: FAL, 800°C preoxidation, upstream surface of media. 200X (T-146-BB-1)

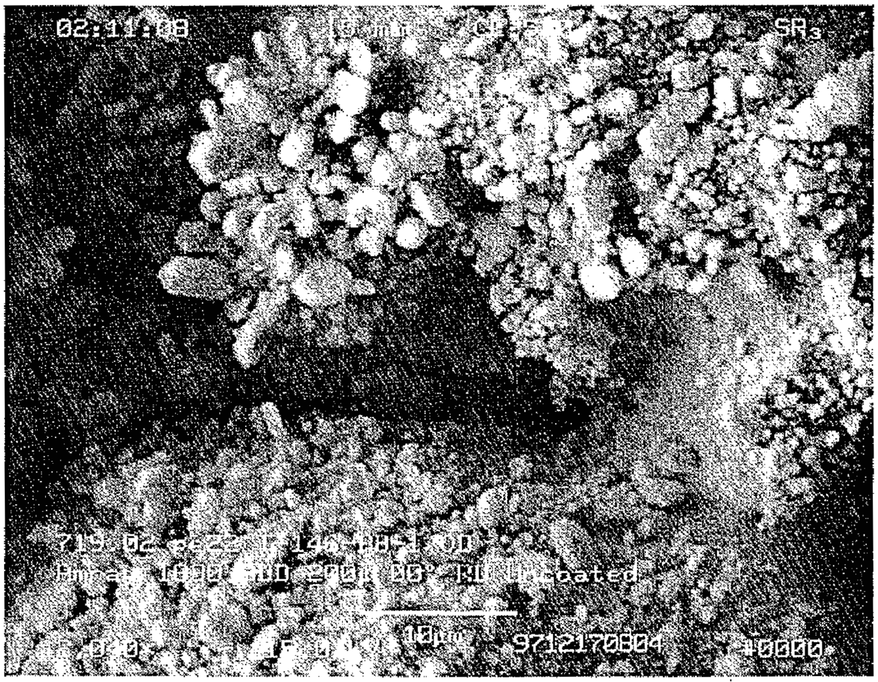

Figure 145: FAL, 800°C preoxidation, upstream surface of media. Small iron and sulfur rich crystals (possibly iron sulfide). 2000X (T-146-BB-1)

Figure 146: FAS, 1000°C preoxidation, upstream surface of media. Crystal is composed of aluminum and zirconium with oxygen (possible Al_2O_3 - ZrO_2), no sulfur. 200X (T-173-C-2)

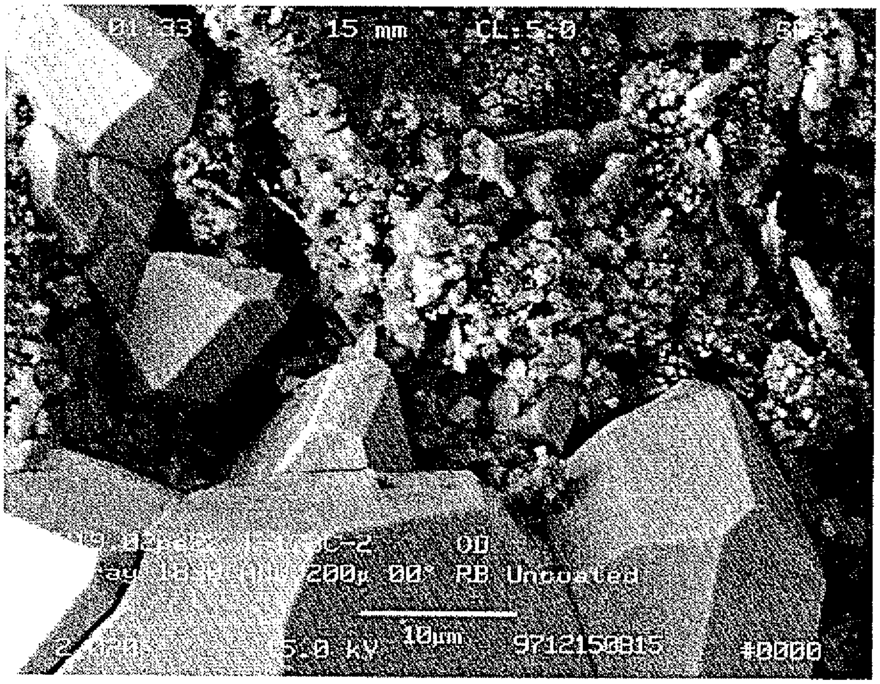

Figure 147: FAS, 1000°C preoxidation, upstream surface of media. Mild sulfur seen with partial field spectrum of surface. 2000X (T-173-C-2)

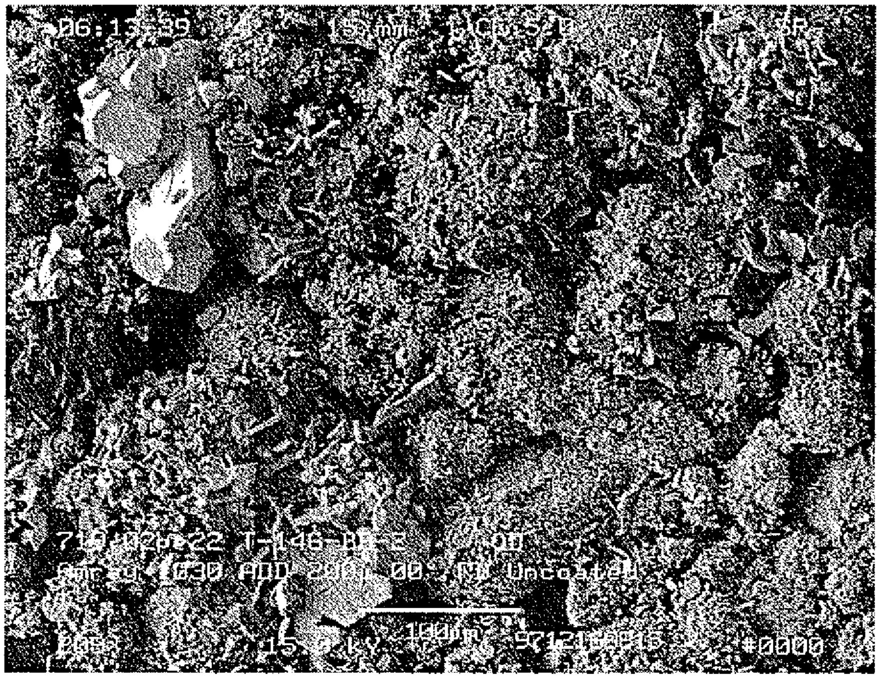

Figure 148: FAL, 1000°C preoxidation, upstream surface of media. Iron sulfide hexagonal crystals. 200X (T-146-BB-2)

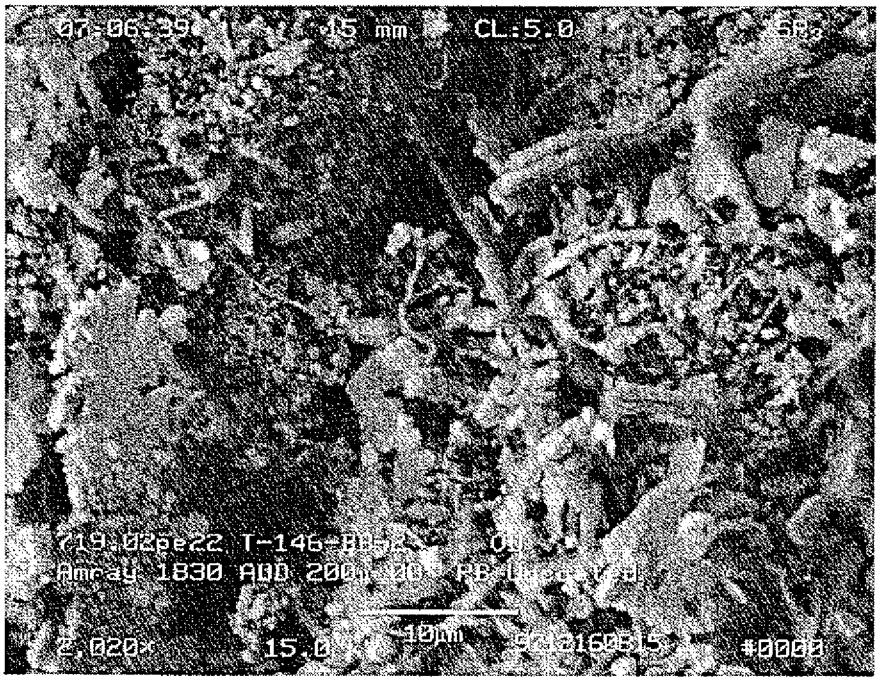

Figure 149: FAL 1000°C preoxidation, upstream surface of media. High sulfur detected using full screen spectrum. 2000X (T-146-BB-2)

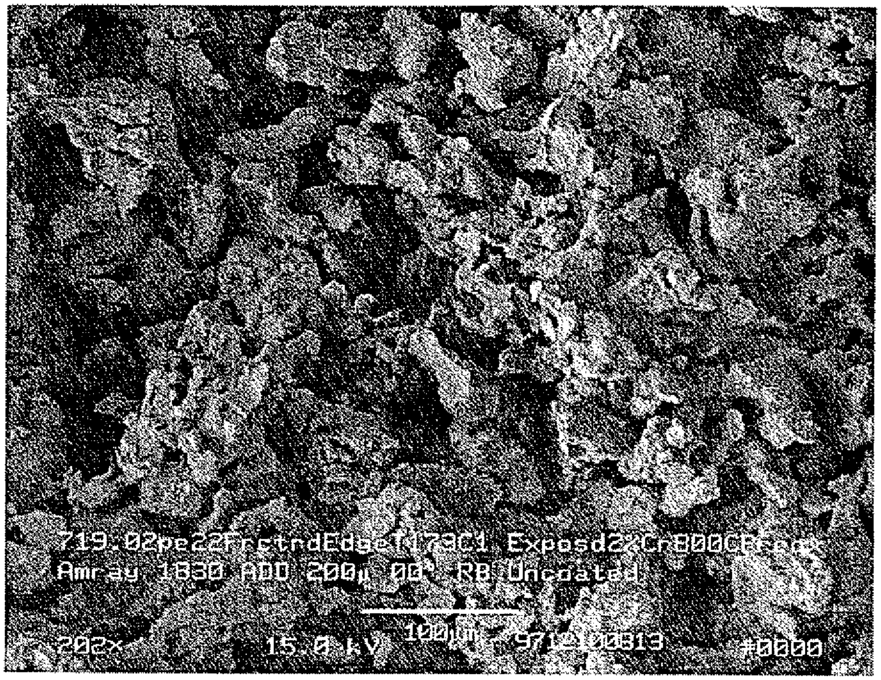

Figure 150: FAS, 800°C preoxidation, exposed, fractured surface. 200X (T-173-C-1)

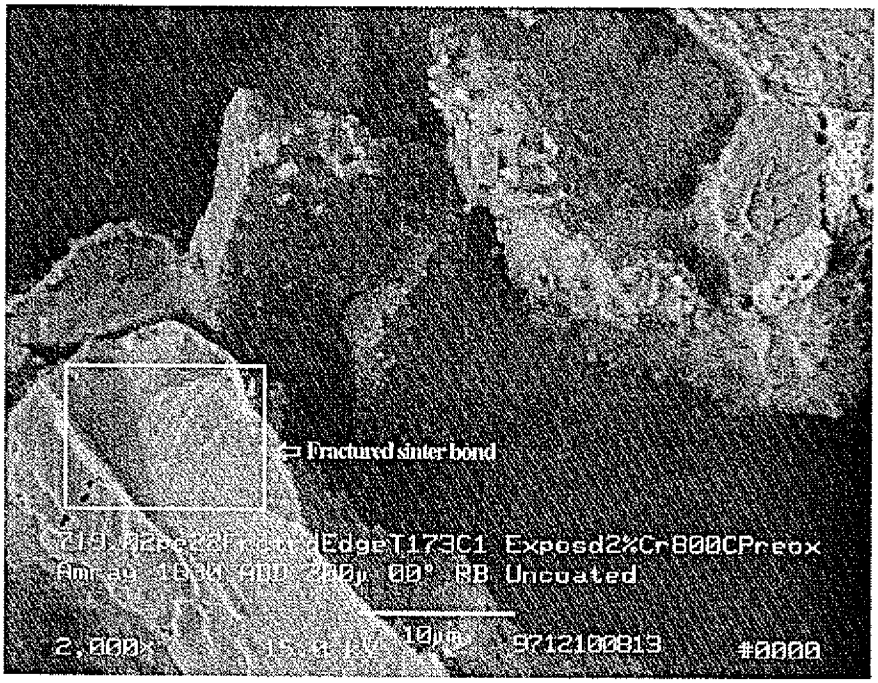

Figure 151: FAS, 800°C preoxidation, exposed, fractured surface. Spectrum and surface morphology are similar to control (Figure 92 and Figure 74). 2000X (T-173-C-1)

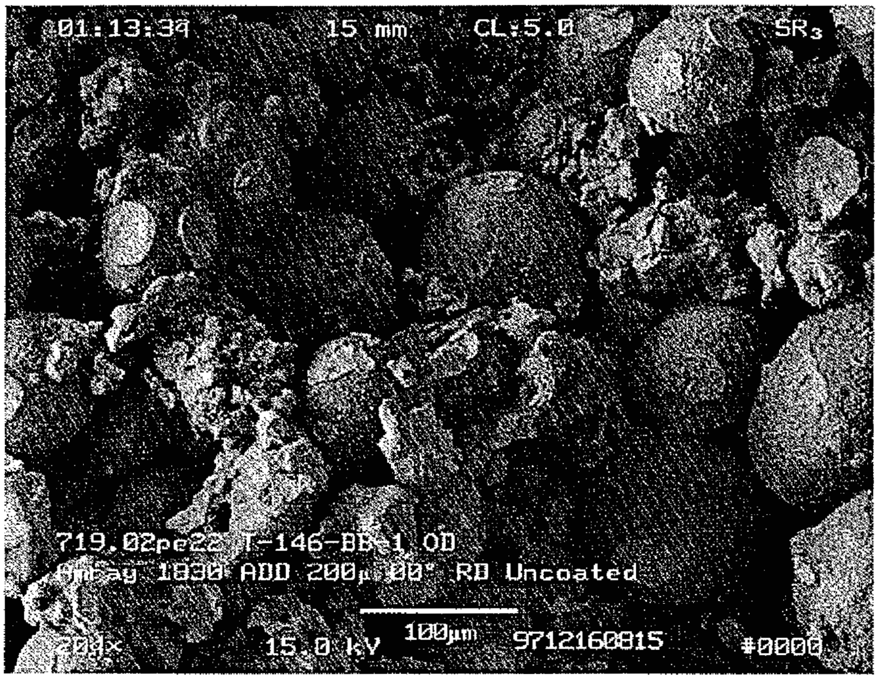

Figure 152: FAL, 800°C preoxidation, exposed, fractured surface. 200X (T-146-BB-1)

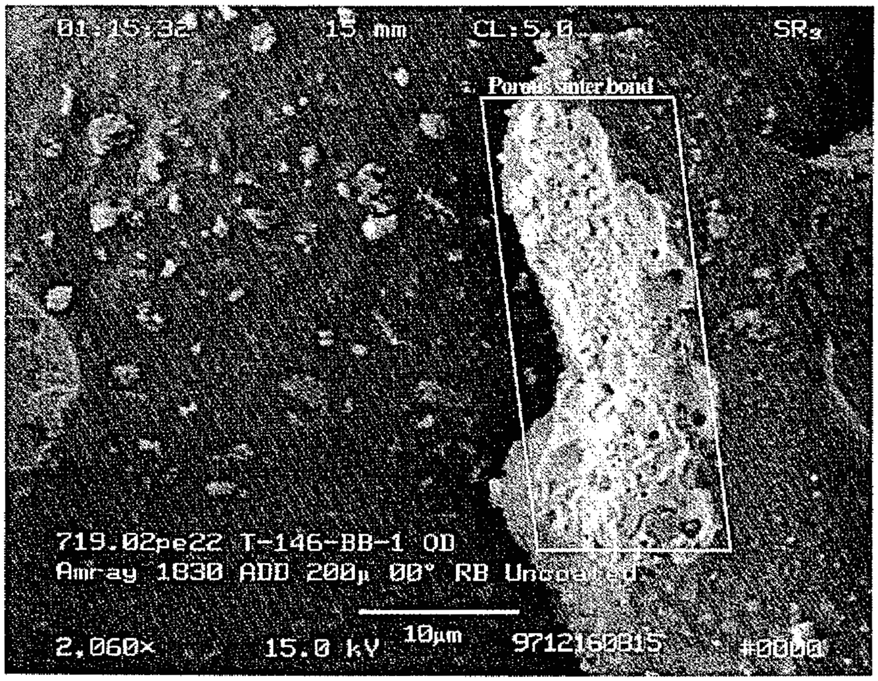

Figure 153: FAL, 800°C preoxidation, exposed, fracture surface. 2000X (T-146-BB-1)

Figure 154: FAS, 1000°C preoxidation, exposed, fractured surface. Significant corrosion. 200X (T-173-C-2)

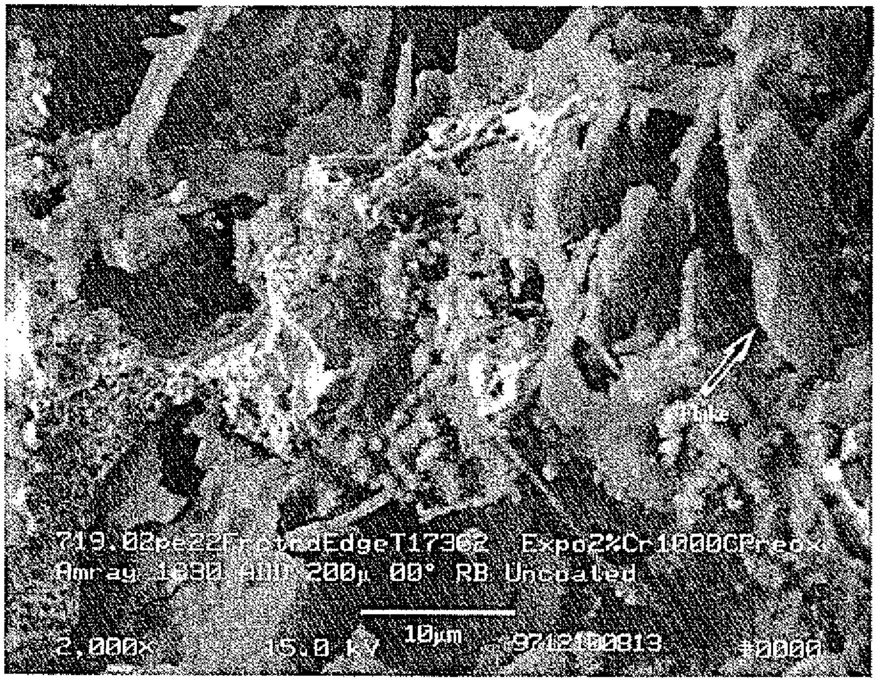

Figure 155: FAS, 1000°C preoxidation, exposed, fractured surface. Mild levels of sulfur detected with full screen spectrum. 2000X (T-173-C-2)

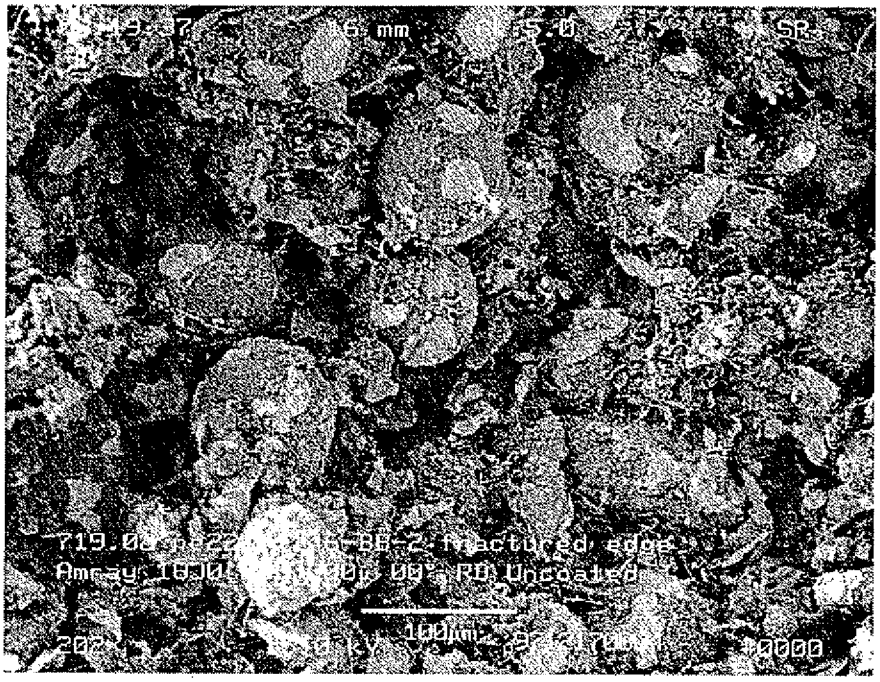

Figure 156: FAL, 1000°C preoxidation, exposed. fractured surface. Large amounts of attack 200X (T-146-BB-2)

Figure 157: FAL, 1000°C preoxidation, exposed, fractured surface. Mild sulfur detected with full screen spectrum. 2000X (T-146-BB-2)

APPENDIX VI: GRAPHS OF LONG-TERM DATA

Non-Destructive Test Results

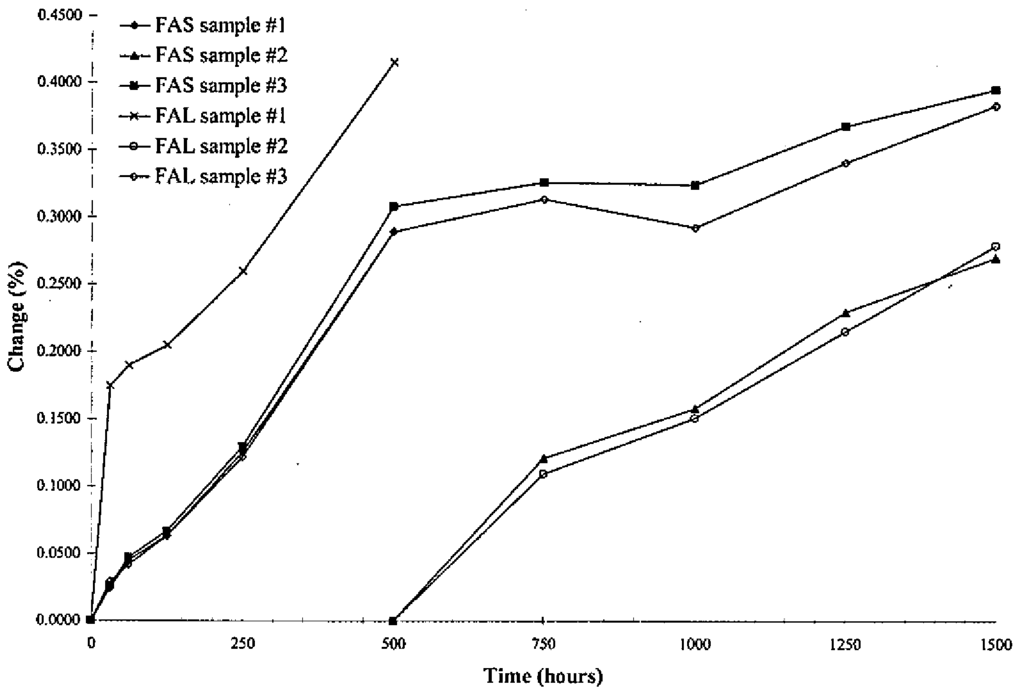

Figure 158: Change in mass of the iron aluminide samples exposed to 7.83 vol.% H_2S at 925°F. These are low mass gains for a porous sample having a total surface area between 5.6 and 6.9 m^2

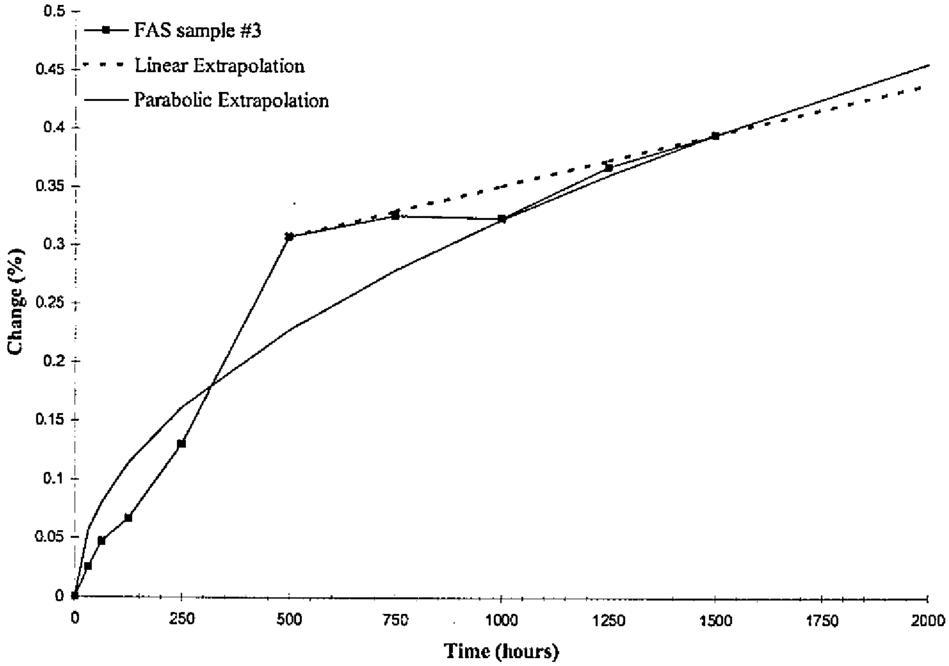

Figure 159: Mass gain extrapolations for FAS sample #3. Both the linear and parabolic fits are shown. Linear fit was done after five-hundred hours of testing.

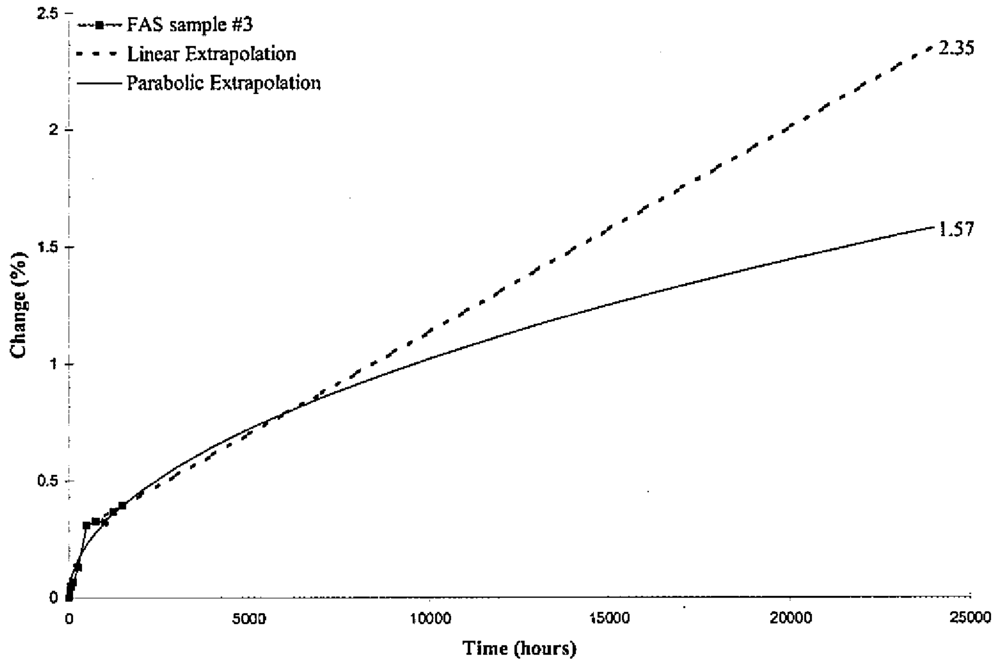

Figure 160: Mass gain extrapolations for FAS sample #3. Both the linear and parabolic fits are shown. The approximated range of mass gains is between 1.57 and 2.35%.

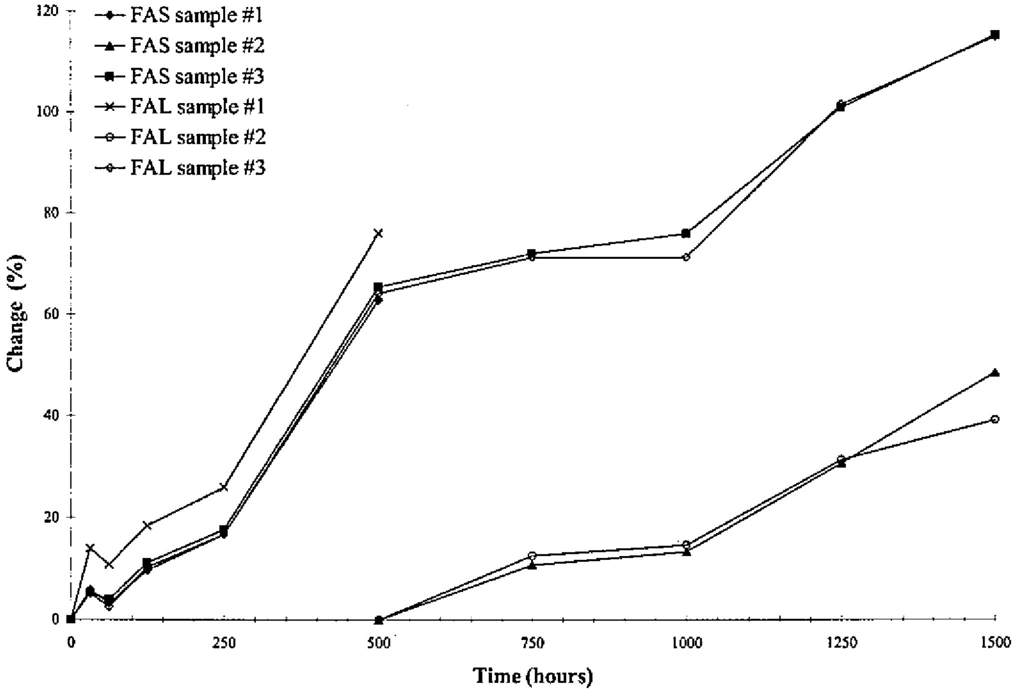

Figure 161: Change in pressure drop of the iron aluminide samples exposed to 7.83 vol.% H_2S at 925°F. These are insignificant increases for a hot gas filter. A permanent ash cake will cause an increase far higher than these.

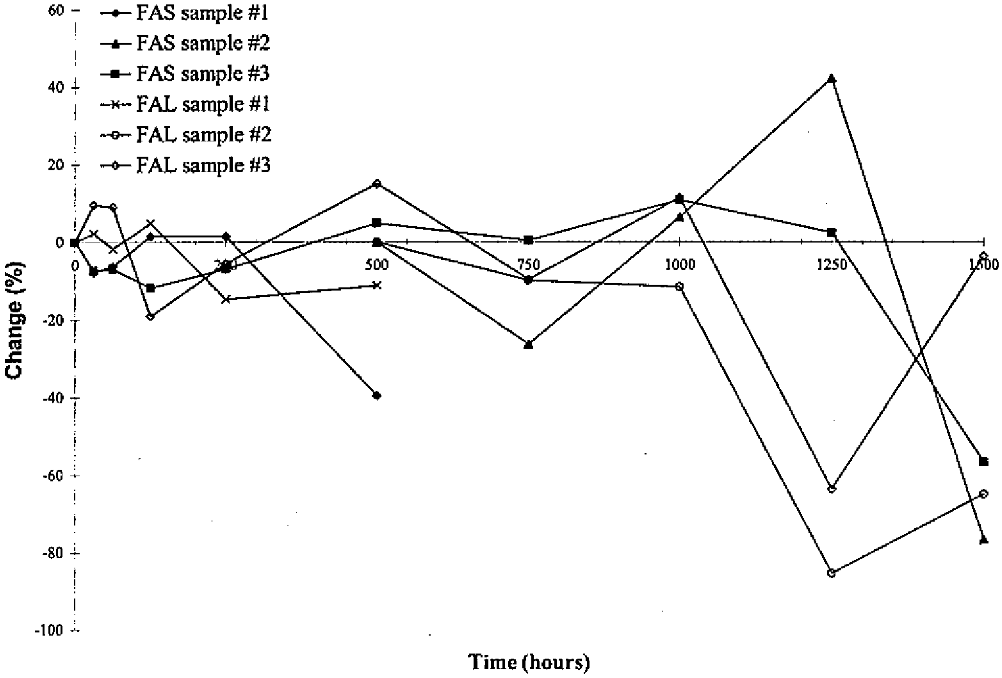

Figure 162: Change in first bubble point of the iron aluminide samples exposed to 7.83 vol.% H_2S at 925°F. These results are inconclusive. Mercury porosimetry provides clearer results.

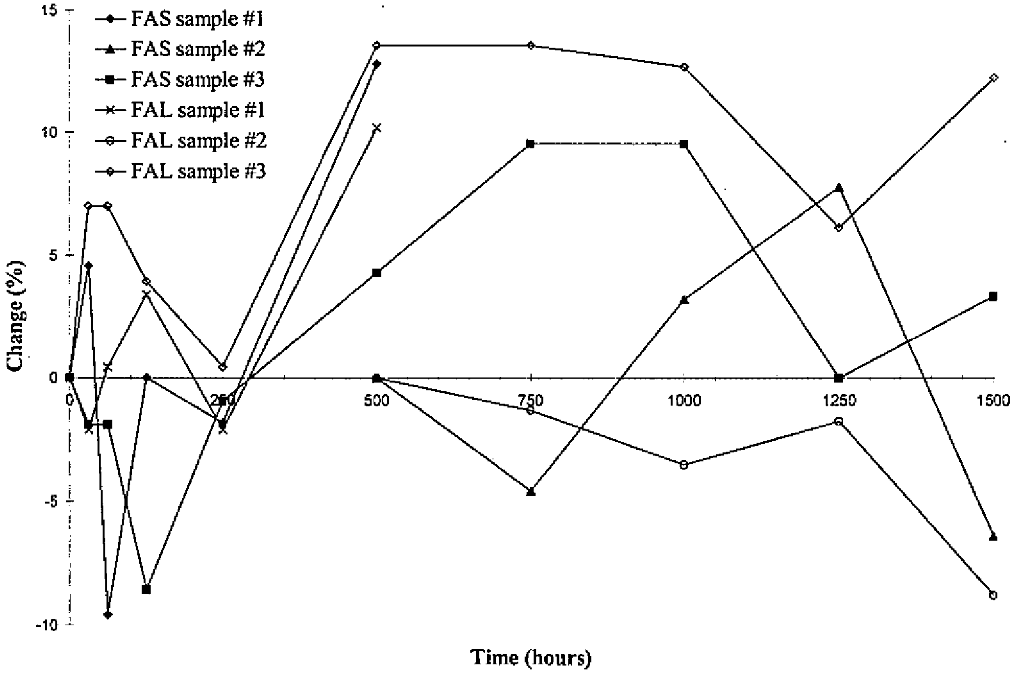

Figure 163: Change in tenth bubble point of the iron aluminide samples exposed to 7.83 vol.% H_2S at 925°F. These results are inconclusive. Mercury porosimetry provides clearer results.

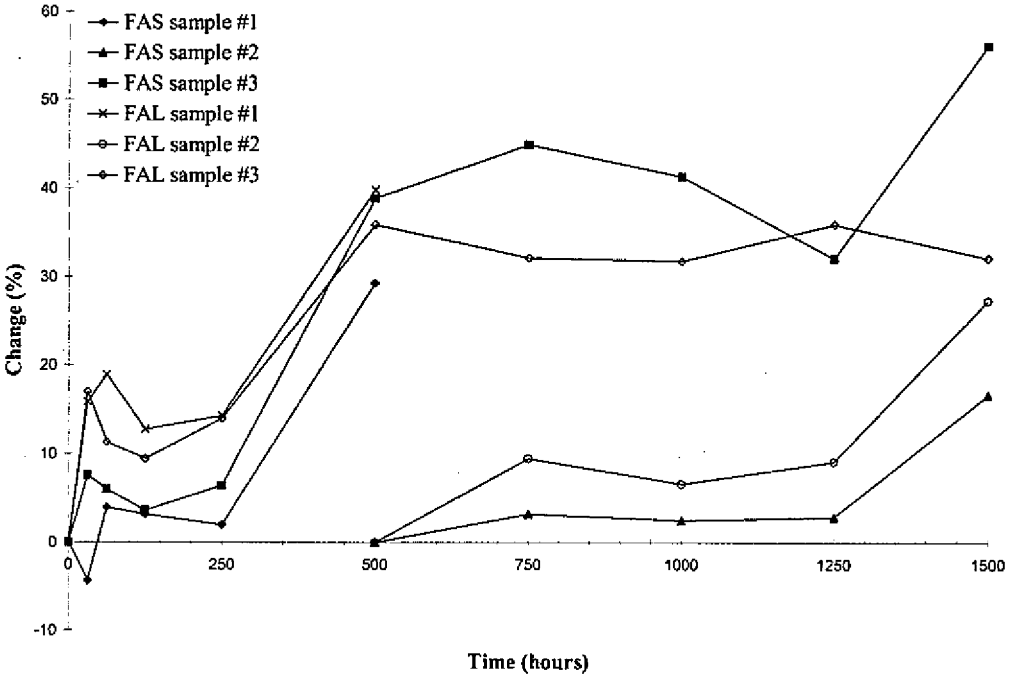

Figure 164: Change in open bubble point of the iron aluminide samples exposed to 7.83 vol.% H_2S at 925°F. An increase indicates a general tightening of the average pore size.

Destructive Test Results

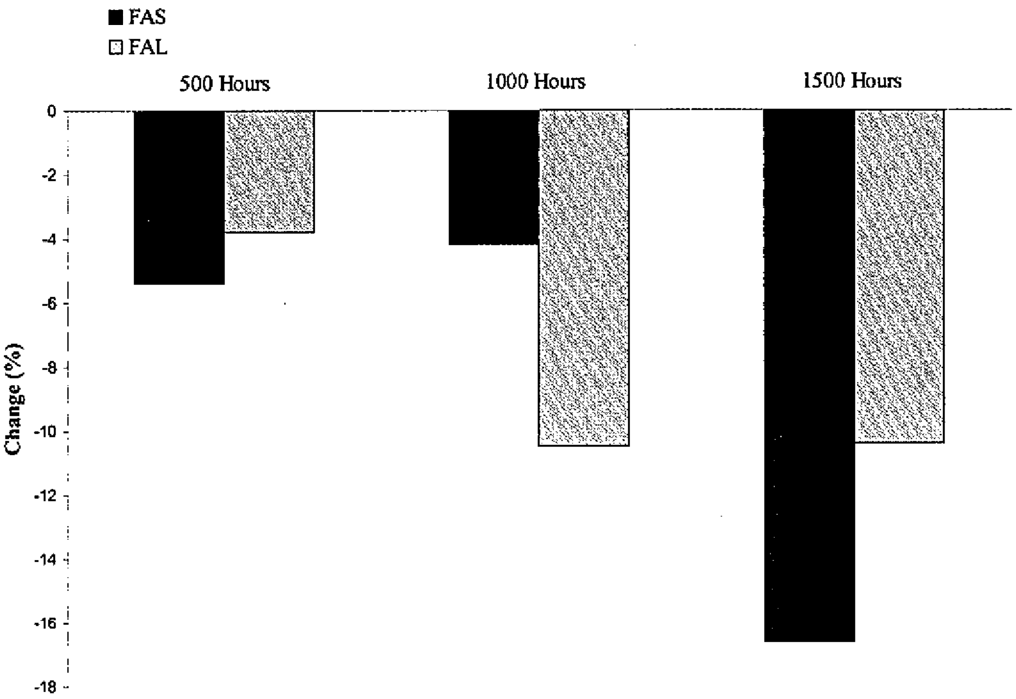

Figure 165: Change in carbon content of the iron aluminide with exposure time. There are only minor changes in the carbon content for both alloys.

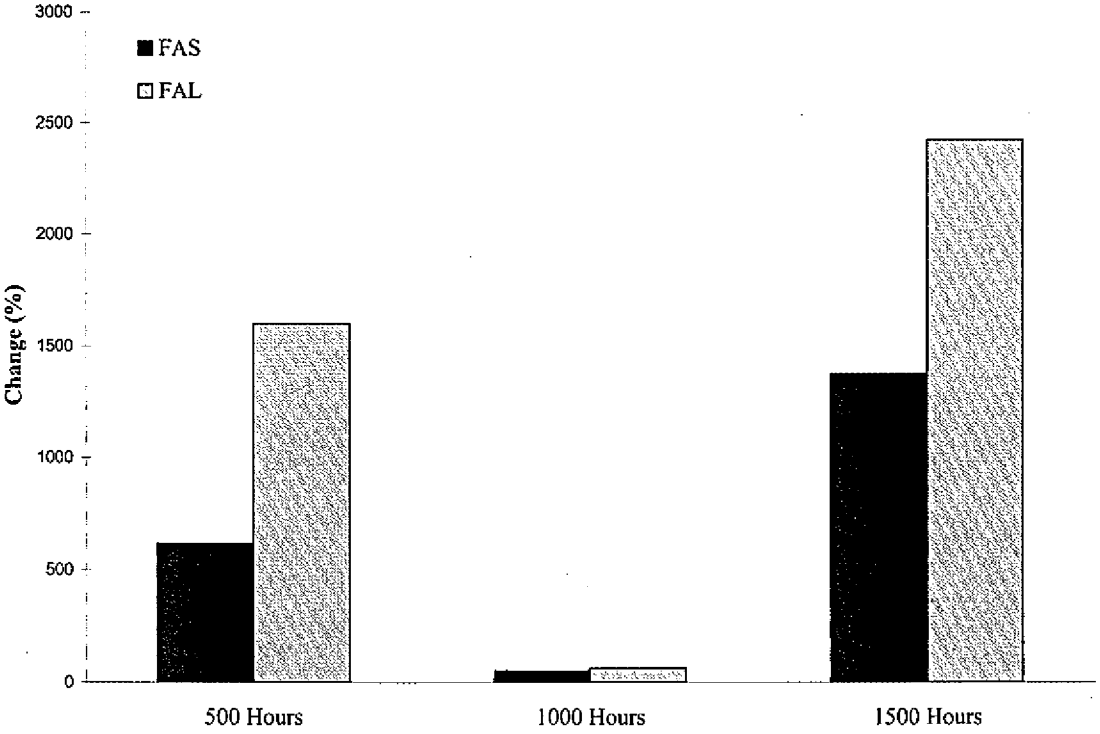

Figure 166: Change in the sulfur content of the iron aluminide alloys. There is a marked increase in the sulfur content of both the alloys.

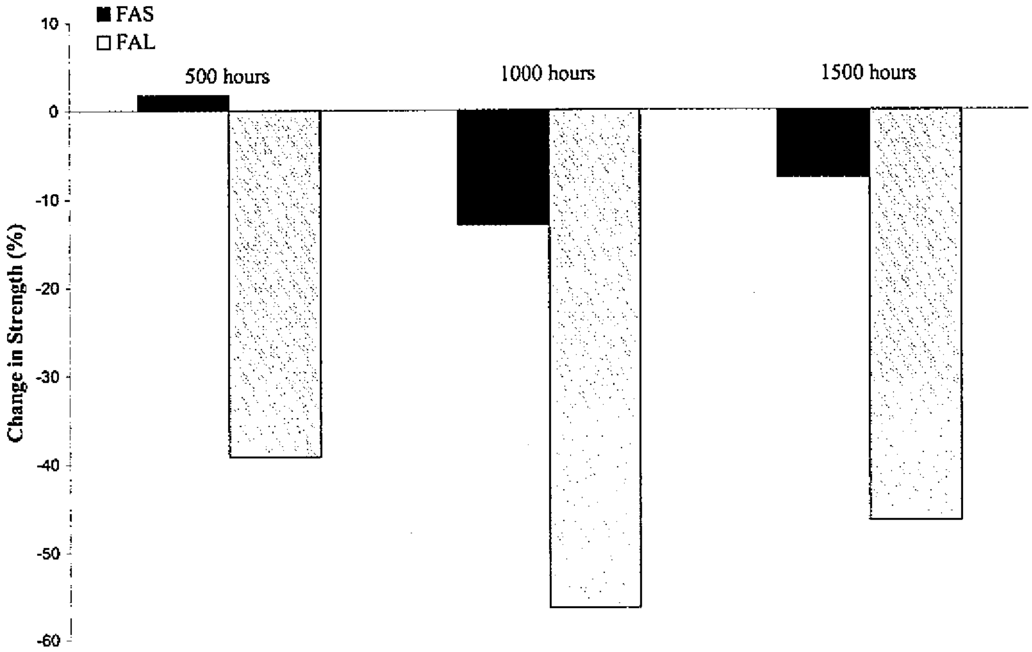

Figure 167: Change in strength of the iron aluminide samples after exposure. The FAS media's strength is unaffected by the exposure to simulated IGCC conditions. The FAL media has a marked decrease in strength, reason currently unknown.

FAS Mercury Porosimetry

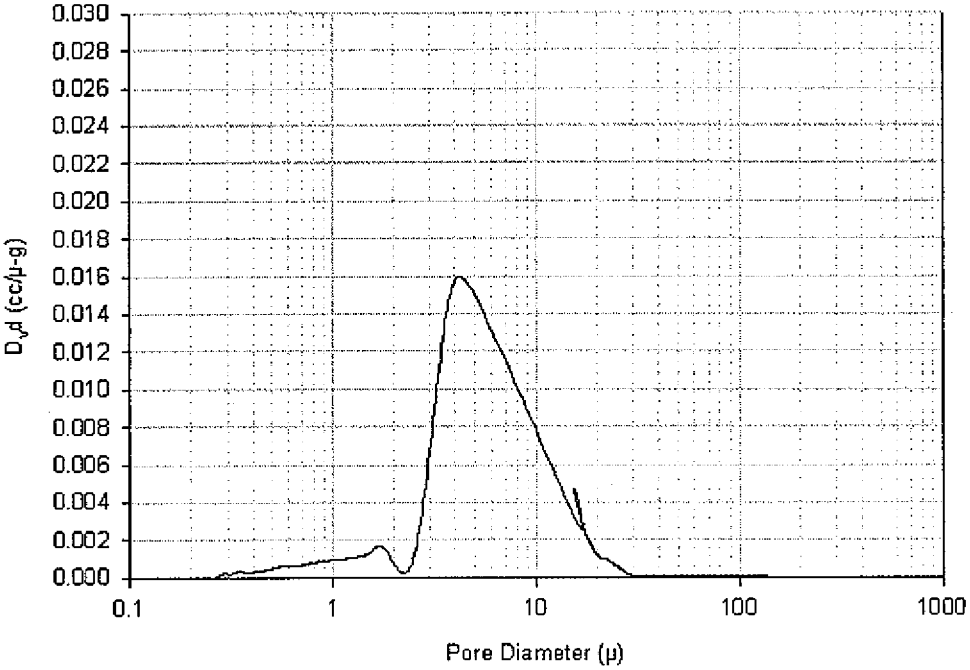

Figure 168: Porosimetry of as-sintered FAS media. Pore distribution centered at approximately 4.5 micron.

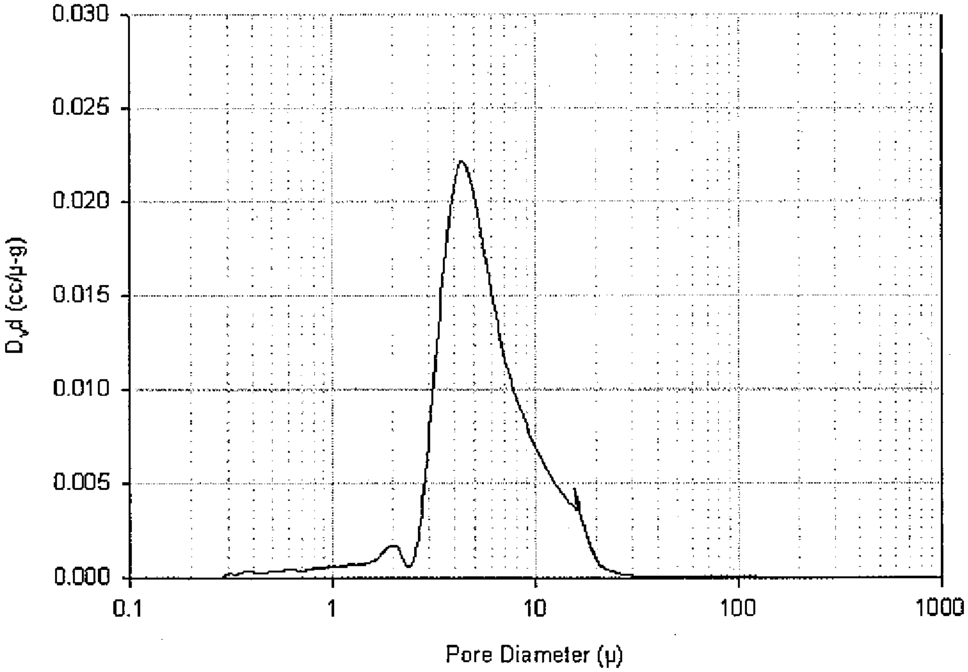

Figure 169: Porosimetry of preoxidized FAS media. Pore distribution centered at approximately 3.5 micron.

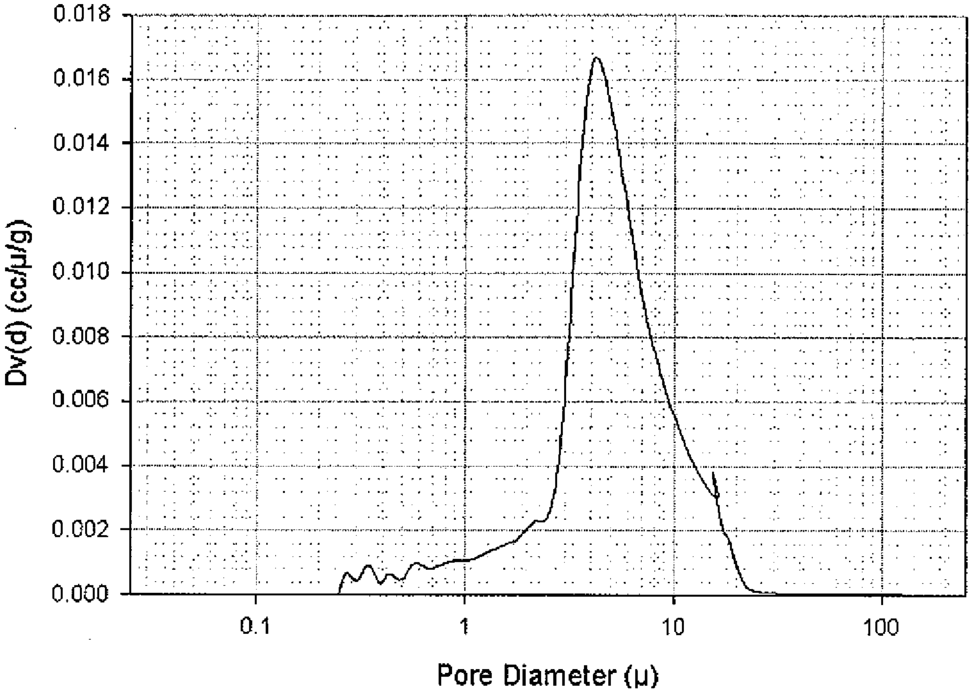

Figure 170: Porosimetry of FAS media exposed for 500 hours. Pore distribution center at approximately 4.0 micron.

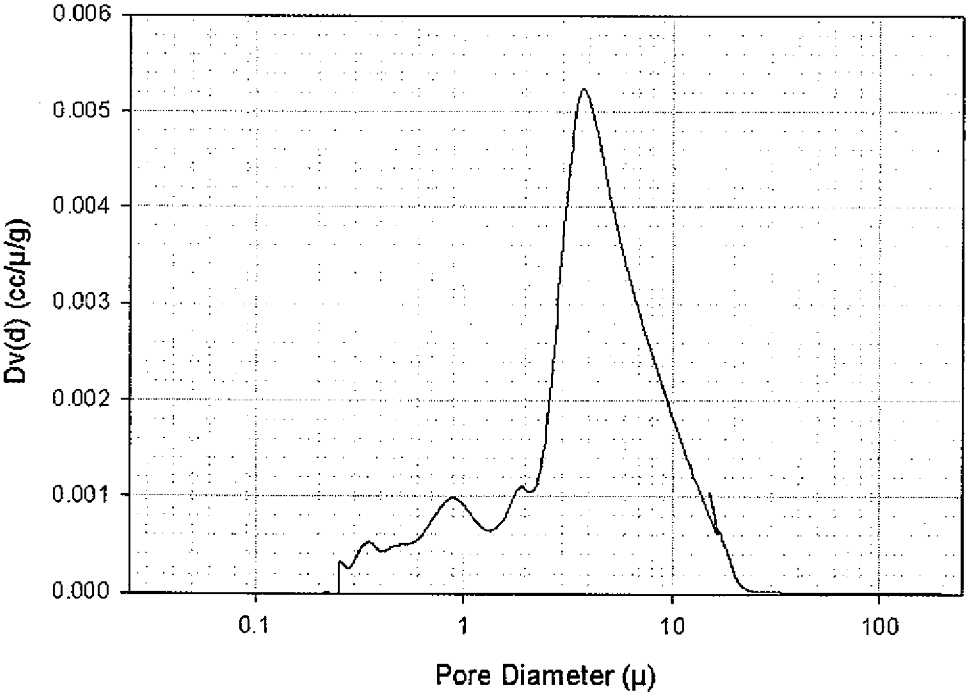

Figure 171: Porosimetry of FAS media exposed for 1000 hours. Pore distribution center at approximately 3.5 micron.

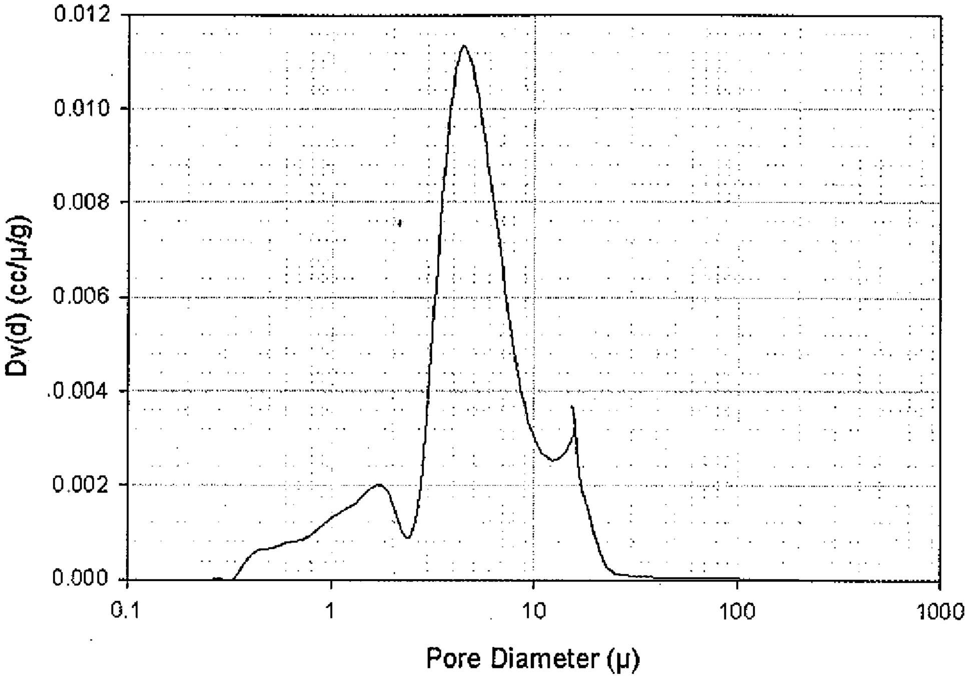

Figure 172: Porosimetry of FAS media exposed for 1500 hours. Pore distribution center at approximately 3.5 micron.

FAL Mercury Porosimetry

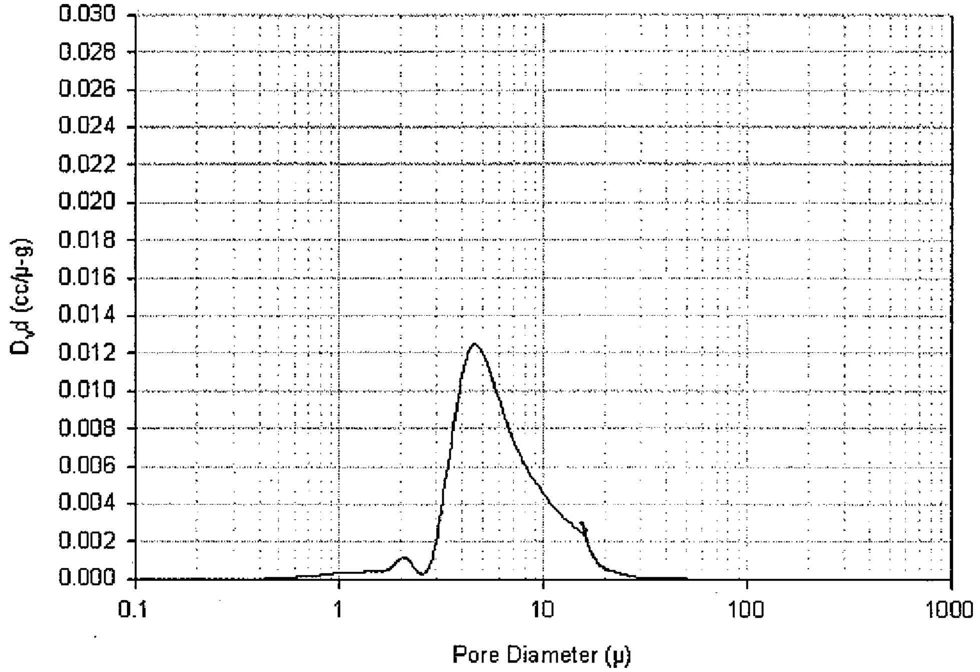

Figure 173: Porosimetry of as-sintered FAL media. Pore distribution centered at approximately 4.5 micron.

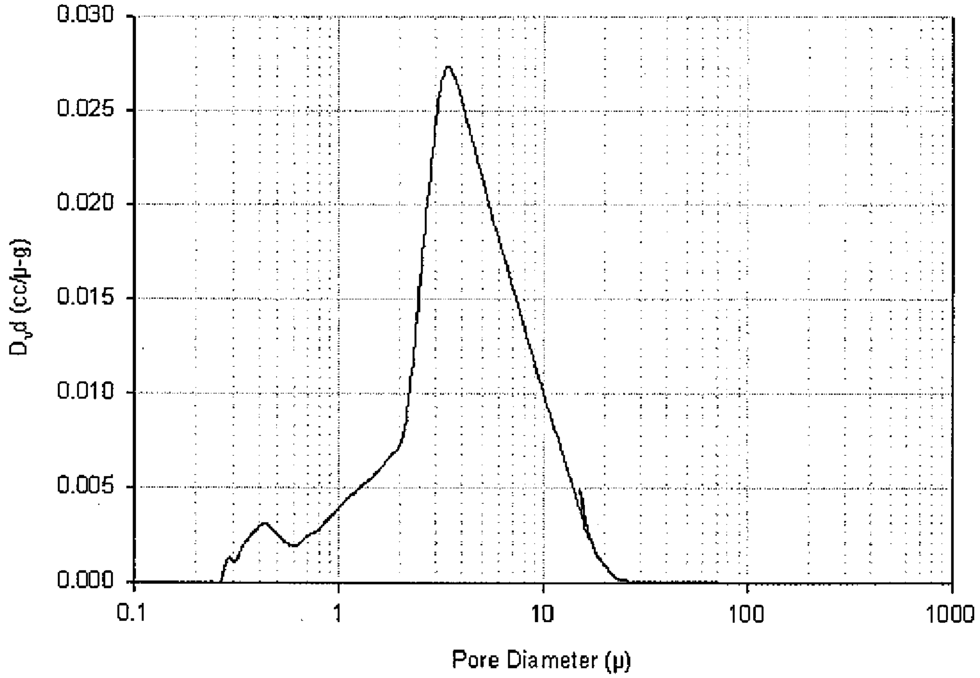

Figure 174: Porosimetry of preoxidized FAL media. Pore distribution centered at approximately 3.5 micron.

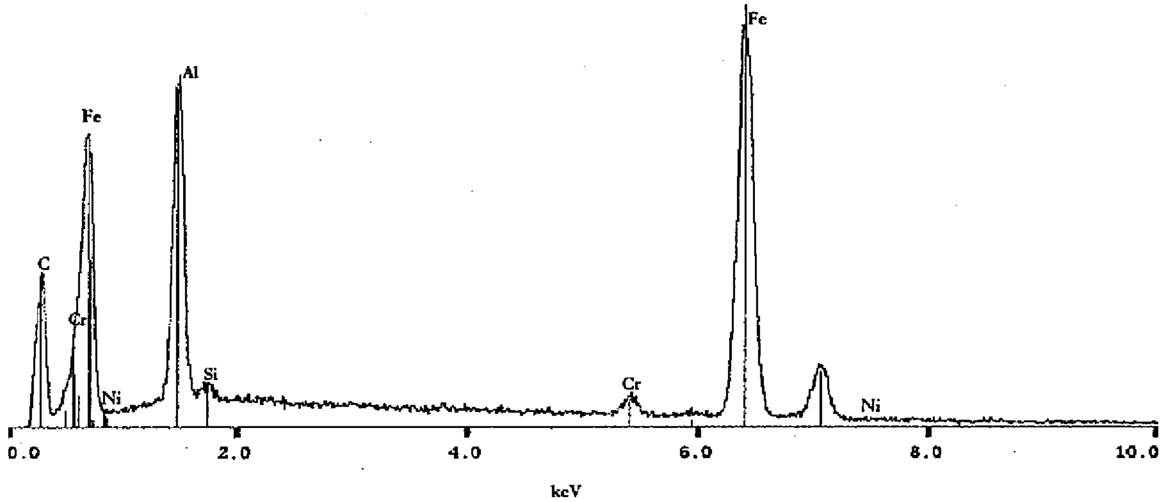

Figure 180: Partial field spectrum of base metal in Figure 179. Typical iron aluminide signature.

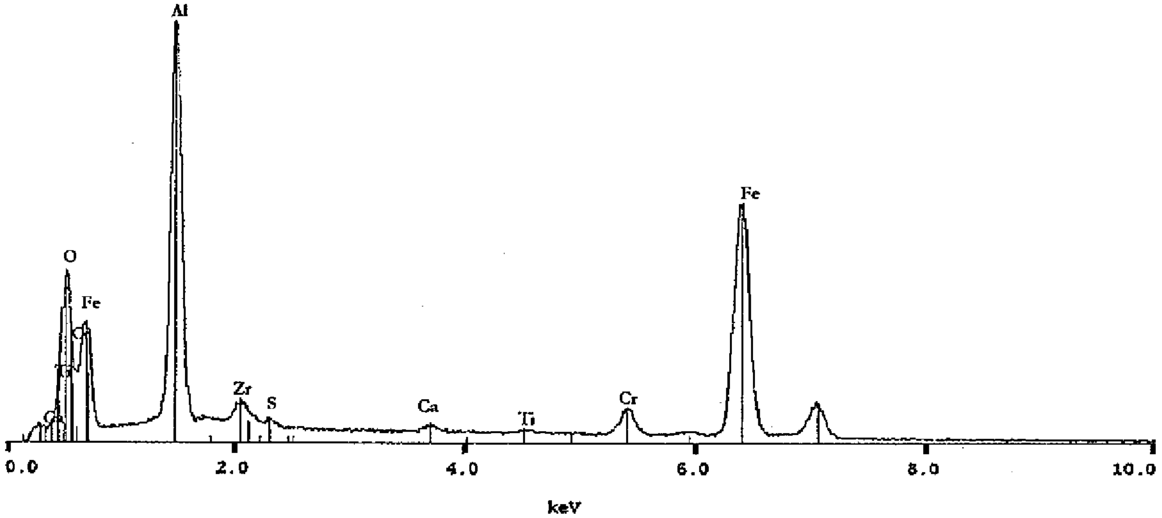

Figure 181: Partial field of upstream surface of Figure 179. Presence of oxygen indicates a thin alumina layer.

Figure 182: Upstream surface of FAS control sample. Preoxidized at 800°C. Sinter bonds between individual powder particles can be seen.

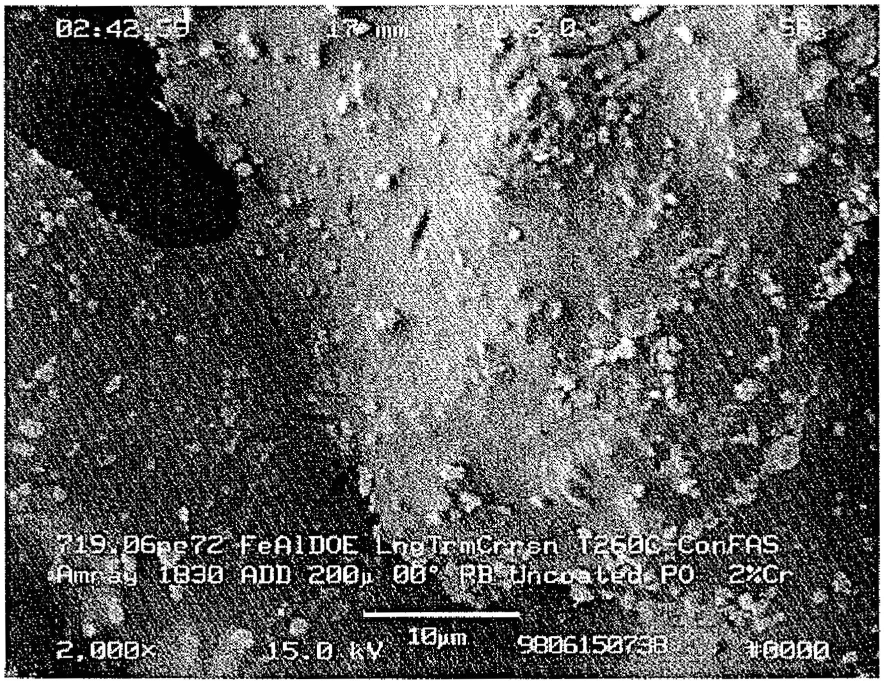

Figure 183: Upstream surface of FAS control sample. Preoxidized at 800°C. Light nodules are zirconia. Typical porous iron aluminide surface.

Figure 186: Fracture surface of FAS control sample. Preoxidized at 800°C. Brittle fracture of an iron aluminide sinter bond is shown. Sinter bond contains a small amount of porosity.

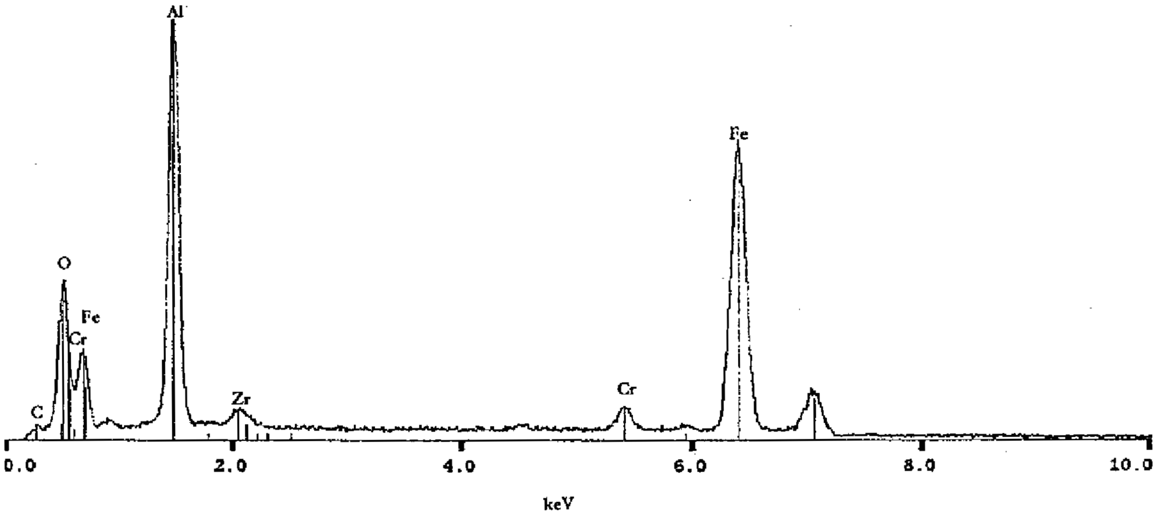

Figure 187: Full screen spectrum of Figure 186. Oxygen peak is from the formation of a continuous aluminum oxide layer.

FAS Sample Exposed for 500 Hours

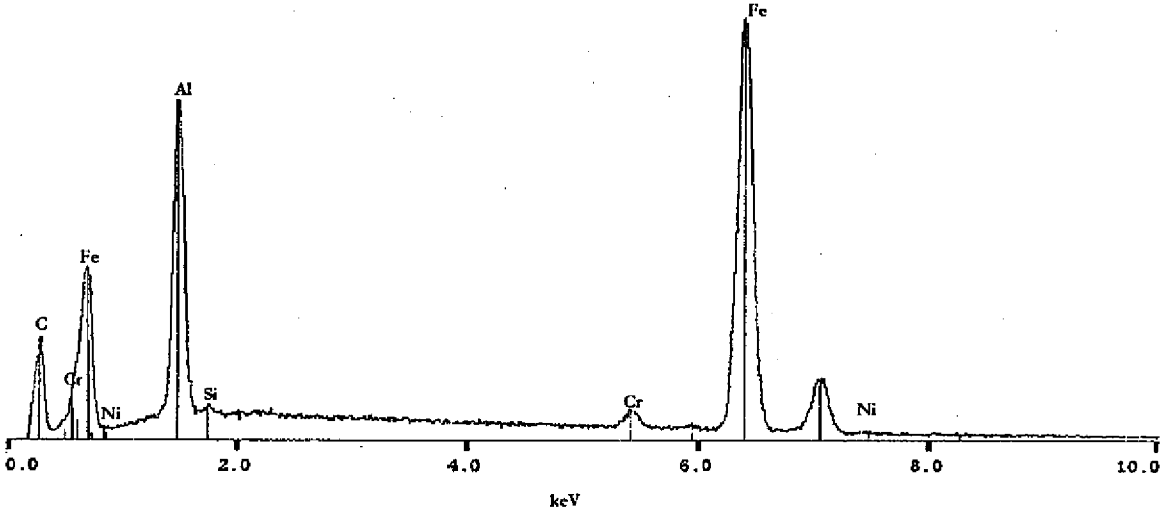

Figure 190: Spectrum of base metal of Figure 189. Typical iron aluminide signature.

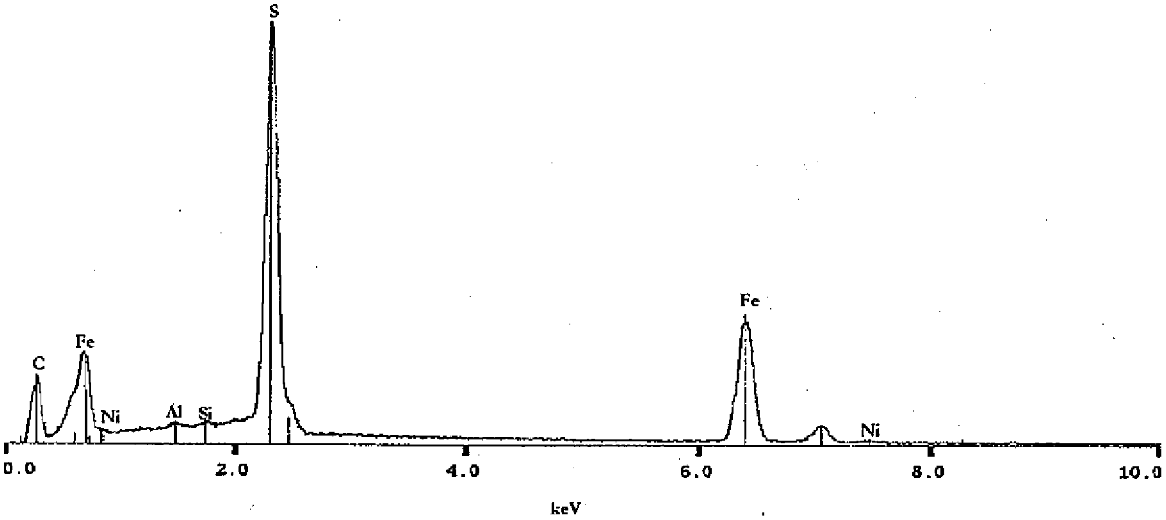

Figure 191: Spectrum of upstream edge of Figure 189. High sulfur peak with iron. A strong indication of iron sulfides.

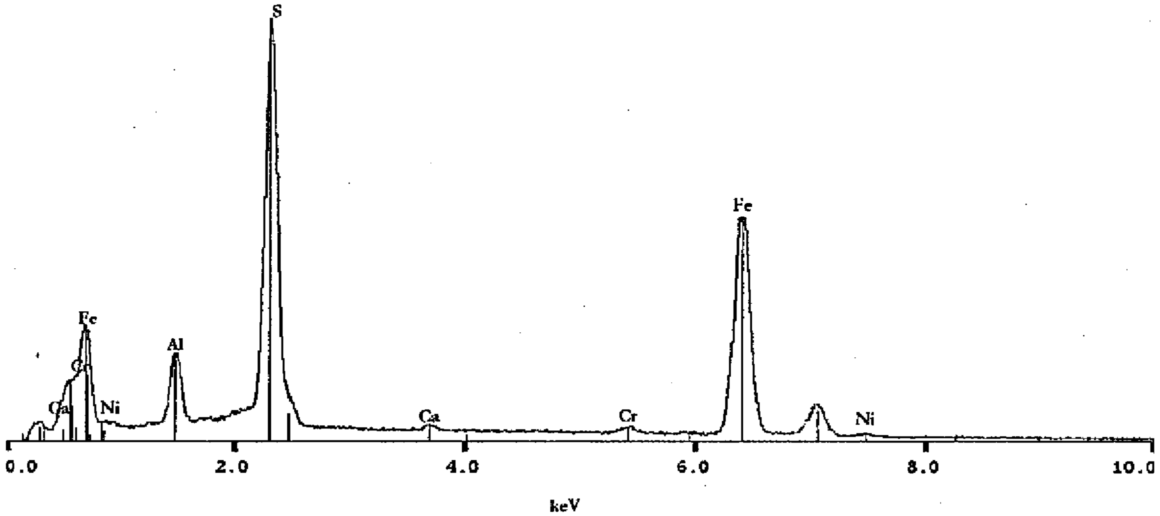

Figure 194: Full screen spectrum of Figure 193. Upstream surface of FAS sample exposed for 500 hours.

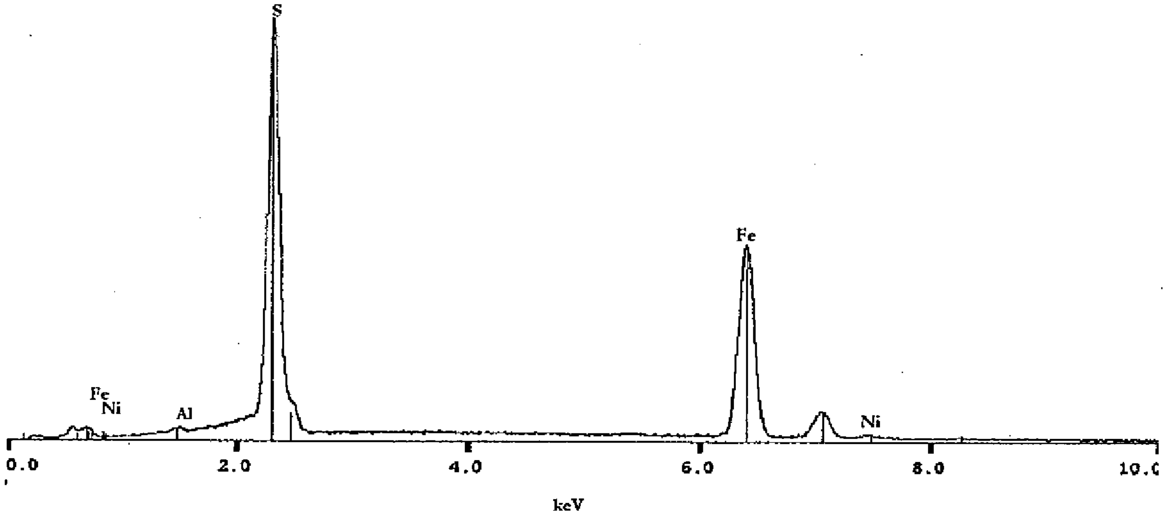

Figure 195: Spot spectrum of crystal structure on surface of Figure 193.

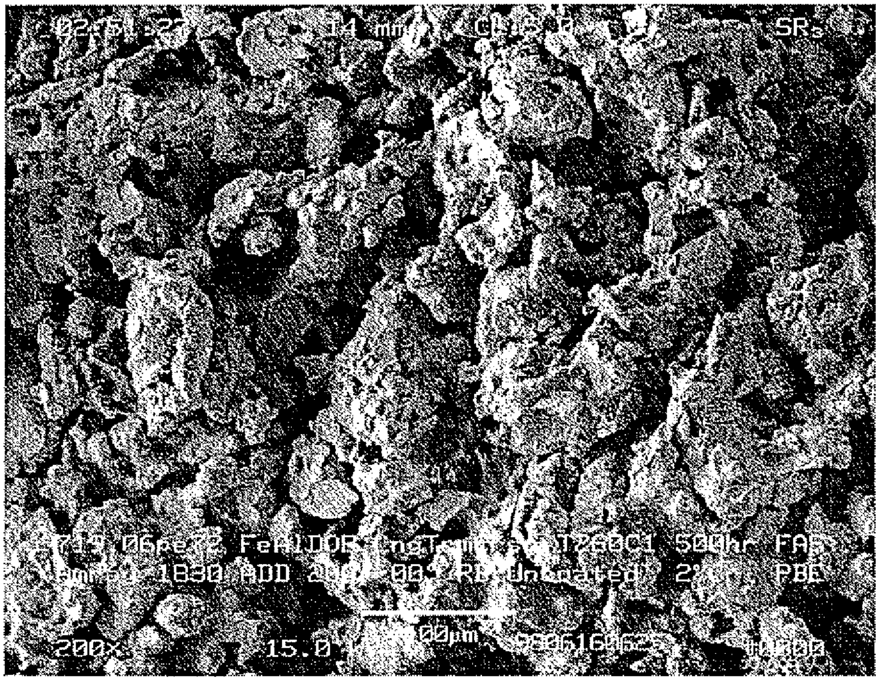

Figure 196: FAS fracture surface. Clean, minimal reaction. Exposed for 500 hours.

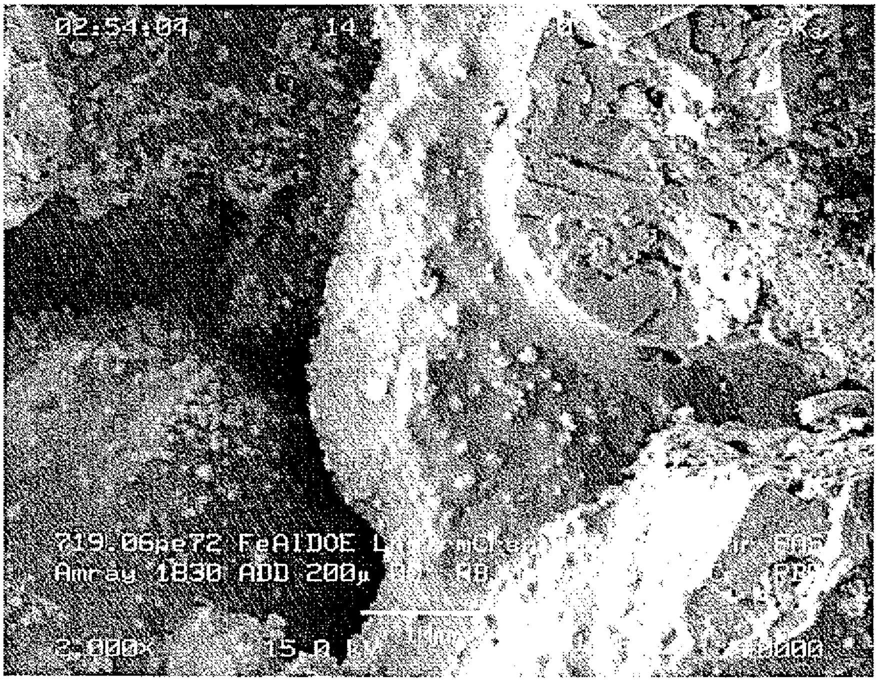

Figure 197: FAS fracture surface. A typical iron aluminide surface. Exposed for 500 hours. Bright zirconium/zirconia nodules on surface.

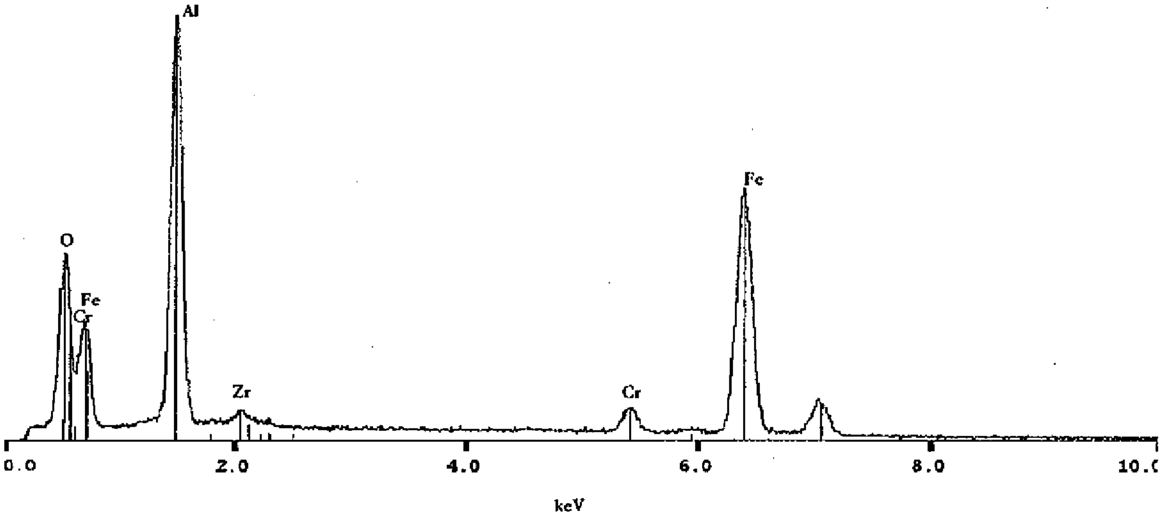

Figure 198: Full screen spectrum of Figure 197. No sulfur present.

FAS Sample Exposed for 1000 Hours

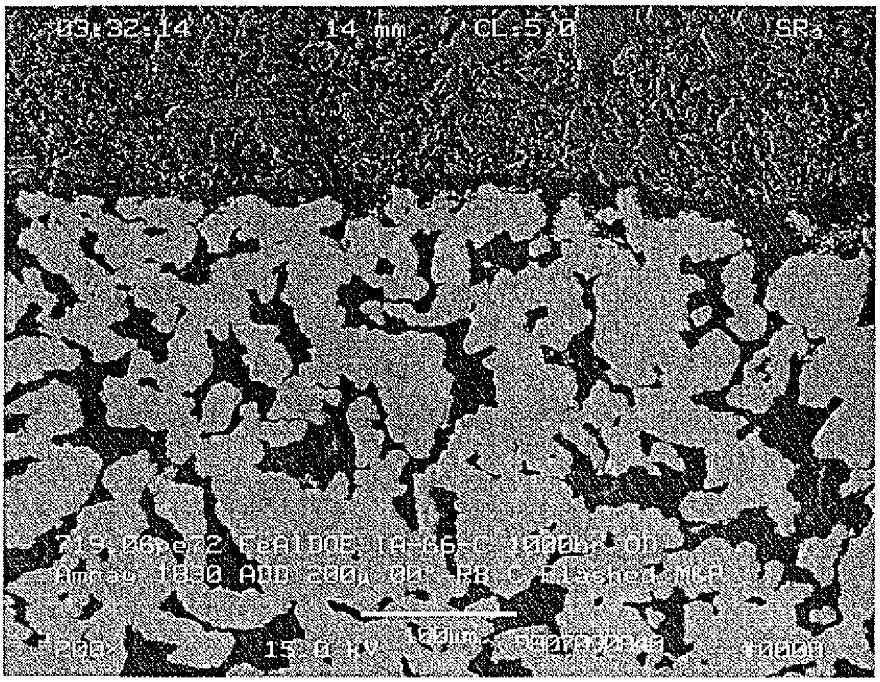

Figure 199: FAS cross-section. Upstream edge shown. Exposed for 1000 hours.

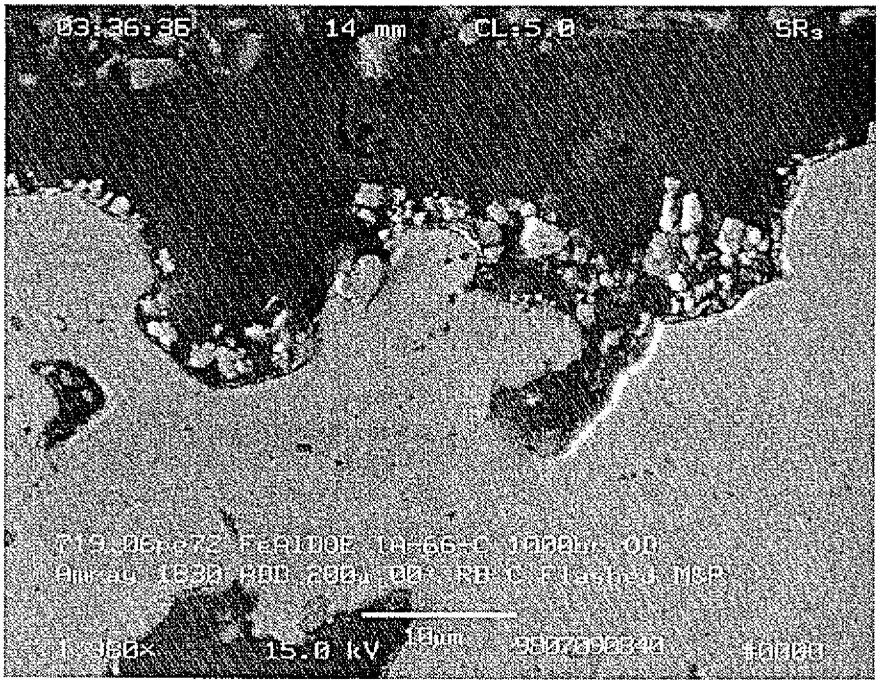

Figure 200: FAS cross-section. Upstream edge shown. Exposed for 1000 hours. Similar iron sulfide crystal formation as seen in Figure 189.

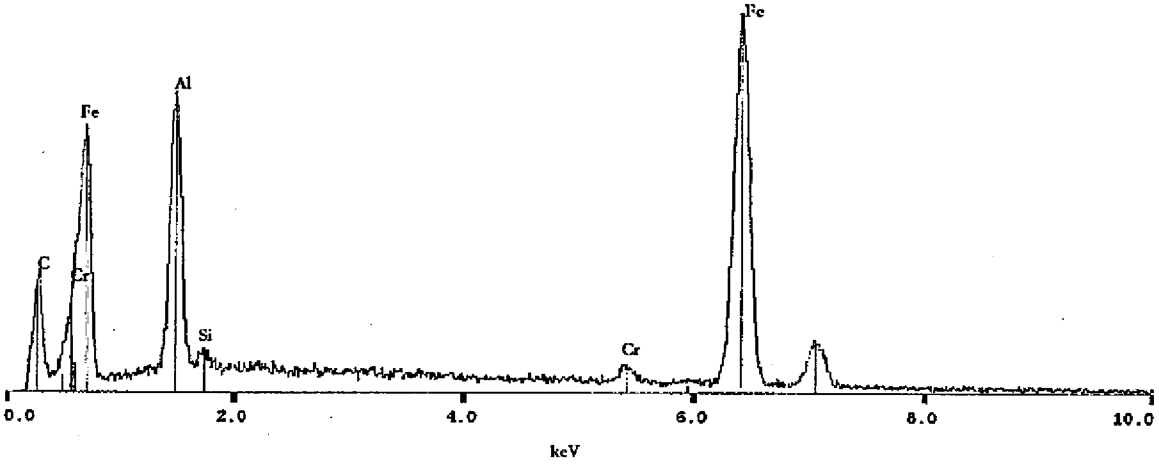

Figure 201: Partial field of base metal in Figure 200. Typical iron aluminide signature. No sulfur penetration.

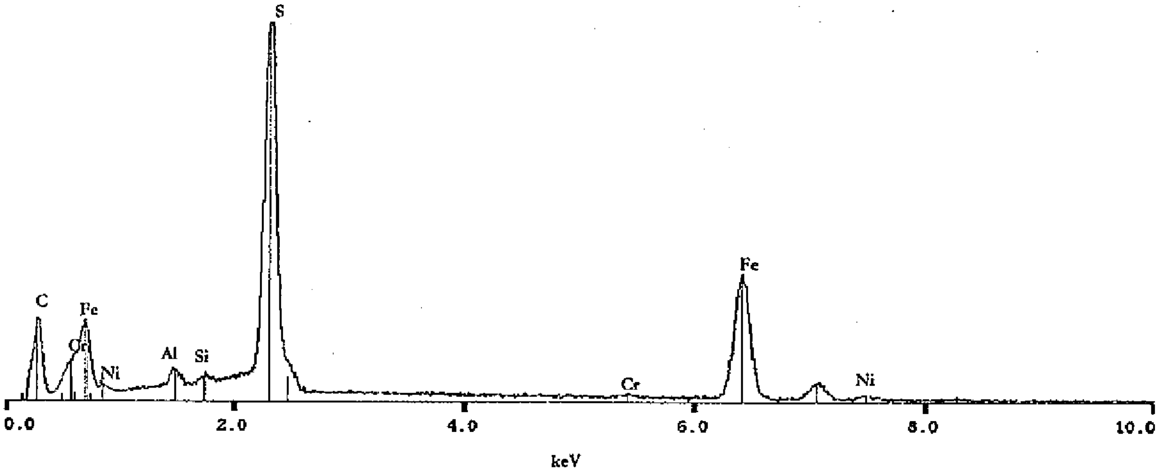

Figure 202: Partial field of upstream edge of Figure 200. High sulfur and iron. A strong indication of iron sulfides.

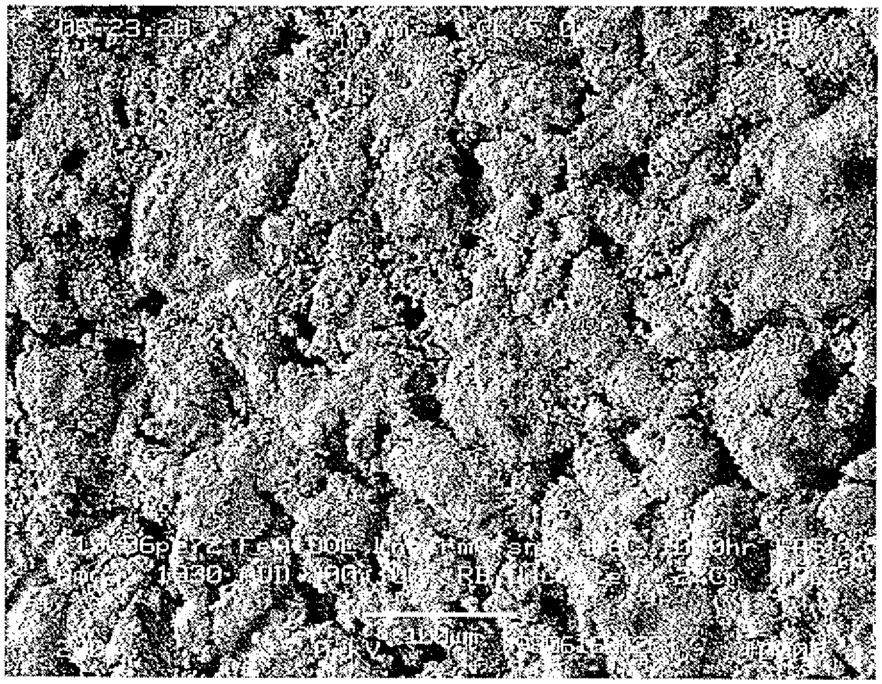

Figure 203: FAS upstream surface. Exposed for 1000 hours. Covered in iron sulfide crystals.

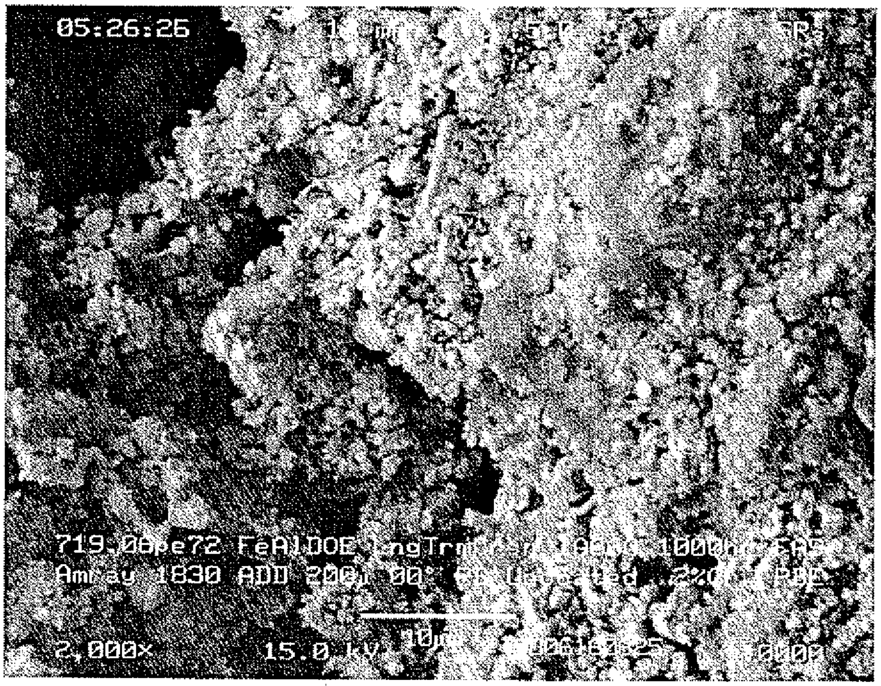

Figure 204: FAS upstream surface. Exposed for 1000 hours.

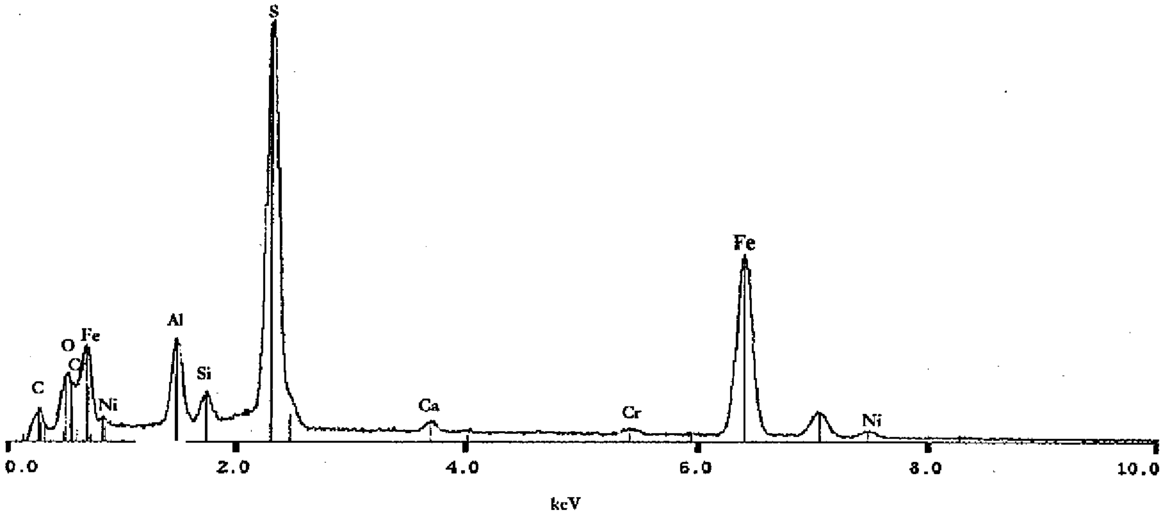

Figure 205: Full screen spectrum of Figure 204. High sulfur and iron. Strong indication of iron sulfide.

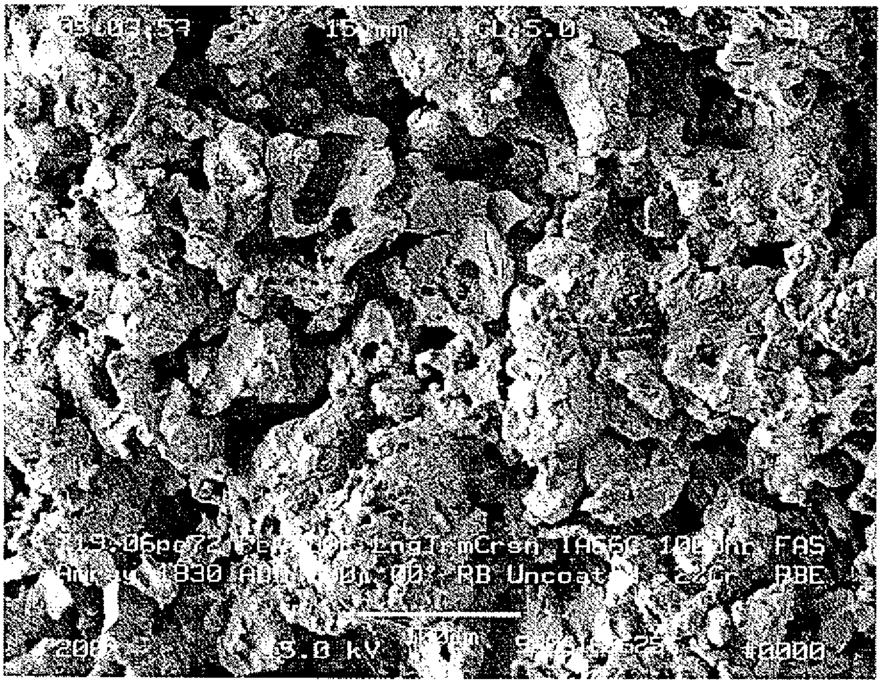

Figure 206: FAS fracture surface. Exposed for 1000 hours.

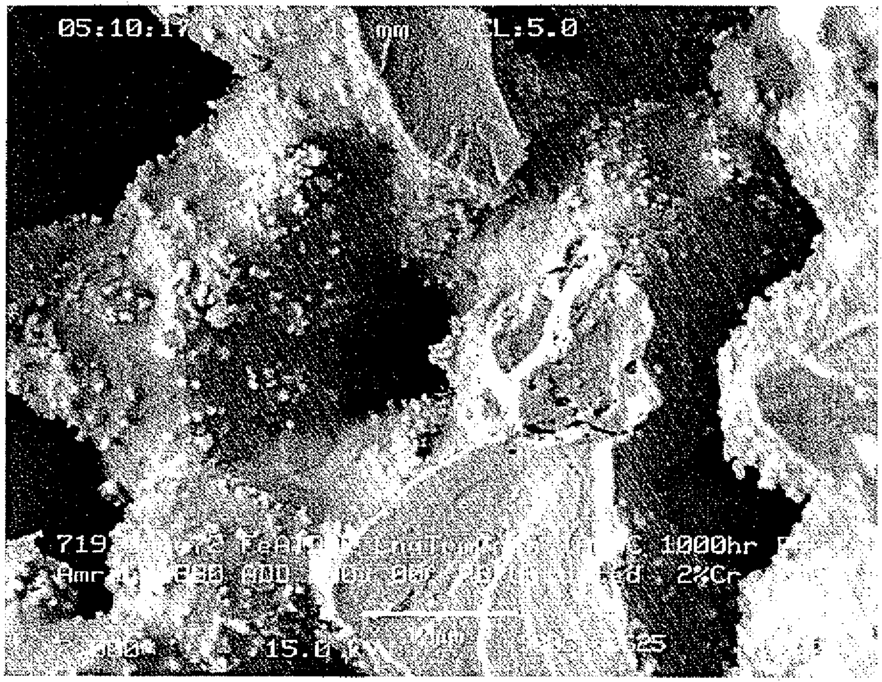

Figure 207: FAS fracture surface. Exposed for 1000 hours. Zirconia nodules, some porosity in the sinter bonds.

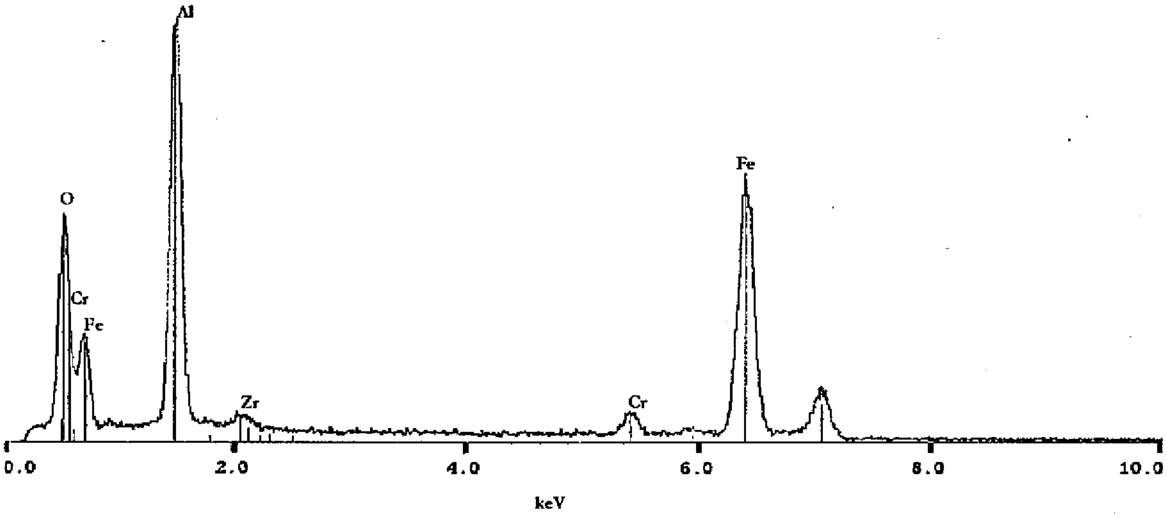

Figure 208: Full screen spectrum of Figure 207. Oxygen peak indicates a thin alumina layer on the surface of the sample.